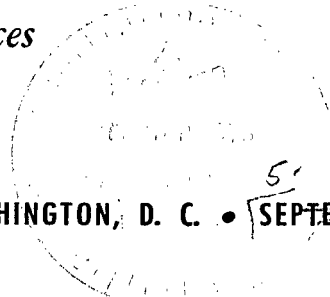# NASA TECHNICAL NOTE

NASA TN D-7972 e./

SUMMARY OF INFORMATION ON LOW-SPEED LATERAL-DIRECTIONAL DERIVATIVES DUE TO RATE OF CHANGE OF SIDESLIP $\dot{\beta}$

*Paul L. Coe, Jr., A. Bruce Graham,
and Joseph R. Chambers*

*Langley Research Center
Hampton, Va. 23665*

and

*The George Washington University
Joint Institute for Acoustics and Flight Sciences
Hampton, Va. 23665*

NATIONAL AERONAUTICS AND SPACE ADMINISTRATION • WASHINGTON, D. C. • SEPTEMBER 1975

1. Report No. NASA TN D-7972	2. Government Accession No.	3. Recipient's Catalog No.
4. Title and Subtitle SUMMARY OF INFORMATION ON LOW-SPEED LATERAL-DIRECTIONAL DERIVATIVES DUE TO RATE OF CHANGE OF SIDESLIP β		5. Report Date September 1975
		6. Performing Organization Code
7. Author(s) Paul L. Coe, Jr., A. Bruce Graham, and Joseph R. Chambers		8. Performing Organization Report No. L-10112
		10. Work Unit No. 505-06-81-01
9. Performing Organization Name and Address NASA Langley Research Center Hampton, Va. 23665		11. Contract or Grant No.
		13. Type of Report and Period Covered Technical Note
12. Sponsoring Agency Name and Address National Aeronautics and Space Administration Washington, D.C. 20546		14. Sponsoring Agency Code

15. Supplementary Notes

16. Abstract

The present paper summarizes the experience obtained by NACA and NASA concerning the low-speed lateral-directional aerodynamic derivatives due to the rate of change of sideslip $\dot{\beta}$, and includes a comprehensive bibliography on this and related subject matter. The results presented show that the magnitudes of the aerodynamic stability derivatives due to rate of change of sideslip become quite large at high angles of attack for swept- and delta-wing configurations, and that such derivatives have large effects on the calculated dynamic stability of these configurations at high angles of attack.

The paper also summarizes the wind-tunnel test techniques used to measure the $\dot{\beta}$ derivatives and discusses various approaches used to predict them. Both the conventional oscillating-airfoil theory and the lag-of-the-sidewash theory are shown to be inadequate for predicting the vertical-tail contribution to the acceleration-in-sideslip derivative $C_{n_{\dot{\beta}}}$; however, a flow-field-lag theory, which is discussed, appears to give qualitative agreement with experimental data for a current twin-jet fighter configuration.

17. Key Words (Suggested by Author(s)) Lateral-directional stability derivatives Acceleration-in-sideslip derivatives Stall/spin High angle of attack	18. Distribution Statement Unclassified – Unlimited Subject Category 08		
19. Security Classif. (of this report) Unclassifed	20. Security Classif. (of this page) Unclassifed	21. No. of Pages 51	22. Price* $4.25

SUMMARY OF INFORMATION ON

LOW-SPEED LATERAL-DIRECTIONAL DERIVATIVES DUE TO

RATE OF CHANGE OF SIDESLIP $\dot{\beta}$

Paul L. Coe, Jr., A. Bruce Graham,[*] and Joseph R. Chambers
Langley Research Center

SUMMARY

The present paper summarizes the experience obtained by NACA and NASA concerning the low-speed aerodynamic stability derivatives due to the rate of change of sideslip $\dot{\beta}$. The report also includes a comprehensive bibliography on this and related subject matter.

The data show that large values of the acceleration-in-sideslip derivatives $C_{n_{\dot{\beta}}}$ and $C_{l_{\dot{\beta}}}$ are obtained for swept- and delta-wing configurations at high angles of attack. The physical flow phenomenon responsible for the $\dot{\beta}$ derivatives is associated with (1) the establishment of leading-edge vortex sheets and flow separation on such wings at high angles of attack; and (2) an increment in the aerodynamic moments, produced by the separated flow, which lags the motion of the configuration. The $\dot{\beta}$ derivatives are found to be very dependent on the frequency of oscillation, with the larger values obtained for the lower frequency.

The paper also shows that the conventional use of rotary forced-oscillation data in the equation of motion to represent derivatives due to pure angular rates is erroneous at high angles of attack, where the $\dot{\beta}$ derivatives are of significant magnitude. In addition, it is shown that the conventional oscillating-airfoil theory and the lag-of-the-sidewash theory are inadequate for predicting the contribution of the vertical tail to $C_{n_{\dot{\beta}}}$. However, a flow-field-lag theory, devised in NACA RM L55H05 and extended herein, is found to yield values of $C_{n_{\dot{\beta}}}$ and $C_{l_{\dot{\beta}}}$ which appear to be in qualitative agreement with experimental data for a current twin-jet fighter configuration.

INTRODUCTION

Recently, concern has arisen over the poor lateral-directional stability and control characteristics exhibited by many current high-performance military airplanes at high

[*]Graduate research assistant, The George Washington University, Joint Institute for Acoustics and Flight Sciences.

angles of attack. These poor characteristics have resulted in an alarming number of inadvertent stalls, post-stall gyrations, and spins, which have produced a significant number of losses of aircraft and aircrews as well as severe operational restrictions. In view of this problem, the National Aeronautics and Space Administration is currently engaged in a broad research program designed to provide fundamental information regarding the aerodynamic characteristics of fighter configurations at high angles of attack. It is intended that such information will serve as a basis for the design of future aircraft which will be either inherently spin resistant or which will use avionics and control-system concepts for automatic spin prevention.

Research conducted by NACA in the 1950's (refs. 1 to 5) indicated that at high angles of attack, the magnitudes of the aerodynamic stability derivatives due to rate of change of sideslip $\dot{\beta}$ became quite large for swept- and delta-wing configurations, and that such derivatives had large effects on the dynamic stability of these configurations. Unfortunately, this research was conducted during a period of time when it was generally believed that future fighter aircraft would be standoff missile launchers, with no requirements for severe maneuvering or the attendant requirement for flight at high angles of attack. Because of an apparent lack of application of this research, the results of the past investigations were fragmented and are therefore generally not considered in current analysis techniques for flight at high angles of attack. Recent military experience, however, has indicated a renewal of close-in, air-to-air combat involving strenuous maneuvering at angles of attack near the stall. The current stall/spin problems reflect this change in operational requirements, and it appears that a reconsideration of past research is required if future stall/spin problems are to be avoided.

The purpose of the present report is to summarize, in some detail, pertinent information produced by NACA and NASA with regard to the derivatives due to rate of change of sideslip, and to emphasize the significance of these derivatives on the dynamic lateral-directional stability characteristics of high-performance swept-wing aircraft at high angles of attack. The report includes (1) a description of wind-tunnel test techniques used to measure the $\dot{\beta}$ derivatives; (2) illustrations of typical results; (3) a discussion of the effects of $\dot{\beta}$ derivatives on dynamic stability characteristics; and (4) a brief description of concepts which might be used to predict the values of such derivatives.

A chronological listing of publications, not included in the reference section, which pertain to the low-speed, lateral-directional dynamic stability derivatives of aircraft is presented.

SYMBOLS

All longitudinal aerodynamic data are presented with respect to the wind system of axes. The lateral-directional aerodynamic data are presented with respect to the body

system of axes, as shown in figure 1, unless otherwise noted. Dimensional values are presented herein in the International System of Units (SI) with equivalent values given parenthetically in the U.S. Customary Units.

a   nondimensional tail length, $\quad -\left(\dfrac{l_V}{\bar{c}_V/2} + 0.5\right)$

b   wing span, m   (ft)

$\bar{c}$ mean aerodynamic chord, m   (ft)

$\bar{c}_V$ mean aerodynamic chord of vertical tail, m   (ft)

C_D drag coefficient, $\quad F_D/q_\infty S$

C_L lift coefficient, $\quad F_L/q_\infty S$

C_l rolling-moment coefficient, $\quad M_X/q_\infty S b$

C_m pitching-moment coefficient, $\quad M_Y/q_\infty S \bar{c}$

C_n yawing-moment coefficient, $\quad M_Z/q_\infty S b$

C_Y side-force coefficient, $\quad F_Y/q_\infty S$

F_D drag force, N   (lbf)

F_L lift force, N   (lbf)

F_Y side force, N   (lbf)

G   unsteady circulation function

I_X moment of inertia about longitudinal body axis, $kg\text{-}m^2$ $(slug\text{-}ft^2)$

I_Z moment of inertia about normal body axis, $kg\text{-}m^2$ $(slug\text{-}ft^2)$

I_{XZ} product of inertia, $kg\text{-}m^2$ $(slug\text{-}ft^2)$

J   unsteady circulation function

k	reduced frequency of oscillation, $\omega b/2V$
k_v	vertical-tail reduced frequency, $\omega \bar{c}_v/2V$
l_v	distance from origin of axis to $\bar{c}_v/4$, m (ft)
M_X	rolling moment, m-N (ft-lbf)
M_Y	pitching moment, m-N (ft-lbf)
M_Z	yawing moment, m-N (ft-lbf)
p	rolling velocity, rad/sec
q_∞	free-stream dynamic pressure, N/m^2 (lbf/ft^2)
r	yawing velocity, rad/sec
S	wing area, m^2 (ft^2)
S_v	vertical-tail area, m^2 (ft^2)
$t_{1/2}$	time required for oscillation to reach half-amplitude, sec
V	velocity, m/sec (ft/sec)
y_o	amplitude of lateral oscillation, m (ft)
α	angle of attack, deg or rad
β	angle of sideslip, deg or rad
$\dot{\beta}$	rate of change of sideslip angle, rad/sec
λ	taper ratio
σ	sidewash angle (positive when effective sideslip at the vertical tail is reduced), deg or rad
ϕ_l, ϕ_n	phase angles associated with separation effects, rad

4

ω frequency of oscillation, rad/sec

$\left(\Delta C_{n_{\dot{\beta}}}\right)_V$ increment of $C_{n_{\dot{\beta}}}$ due to vertical tail

$\left(\Delta C_{Y_{\dot{\beta}}}\right)_V$ increment of $C_{Y_{\dot{\beta}}}$ due to vertical tail

Subscripts:

k   quantity measured under oscillatory conditions

s   stability-axes data

exp   experimental values obtained under static conditions

theo   theoretical

Stability derivatives:

$$C_{l_\beta} = \frac{\partial C_l}{\partial \beta} \qquad\qquad C_{n_\beta} = \frac{\partial C_n}{\partial \beta} \qquad\qquad C_{Y_\beta} = \frac{\partial C_Y}{\partial \beta}$$

$$C_{l_p} = \frac{\partial C_l}{\partial \frac{pb}{2V}} \qquad\qquad C_{n_p} = \frac{\partial C_n}{\partial \frac{pb}{2V}} \qquad\qquad C_{Y_p} = \frac{\partial C_Y}{\partial \frac{pb}{2V}}$$

$$C_{l_r} = \frac{\partial C_l}{\partial \frac{rb}{2V}} \qquad\qquad C_{n_r} = \frac{\partial C_n}{\partial \frac{rb}{2V}} \qquad\qquad C_{Y_r} = \frac{\partial C_Y}{\partial \frac{rb}{2V}}$$

$$C_{l_{\dot{\beta}}} = \frac{\partial C_l}{\partial \frac{\dot{\beta}b}{2V}} \qquad\qquad C_{n_{\dot{\beta}}} = \frac{\partial C_n}{\partial \frac{\dot{\beta}b}{2V}} \qquad\qquad C_{Y_{\dot{\beta}}} = \frac{\partial C_Y}{\partial \frac{\dot{\beta}b}{2V}}$$

BACKGROUND

    In the analysis of dynamic stability and control characteristics of airplanes, the lateral-directional stability derivatives due to $\dot{\beta}$ have traditionally been neglected because (1) the magnitudes of such derivatives were estimated to be small for the low values of angle of attack associated with the conventional flight envelope; and (2) little information was available regarding the magnitudes of the derivatives at high angles of attack. As will

5

be discussed, it was recognized that a lag of the sidewash at the vertical-tail location tended to increase aerodynamic damping in a manner similar to the lag of downwash for the longitudinal case; however, the lag of the sidewash did not appear to have large effects at low angles of attack for configurations under consideration at that time.

As pointed out in reference 6, in the early 1950's, several cases arose in which total disagreement existed between theoretical predictions of lateral-directional stability characteristics of certain swept-wing configurations and experimental results obtained during flight tests of dynamically scaled free-flight models and actual airplanes at high angles of attack. In these cases, theoretical methods generally predicted very unstable Dutch roll motions whereas flight tests showed highly damped stable motions. Subsequently, wind-tunnel test techniques devised to measure dynamic stability derivatives identified large values of $\dot{\beta}$ derivatives at high angles of attack, which, when used in the equations of motion, produced good agreement with flight tests.

These wind-tunnel studies identified two principal sources of the $\dot{\beta}$ derivatives at high angles of attack: lag of sidewash at the vertical-tail location and lag of flow separation and attachment on highly swept wings. In both situations, the time lags involved in flow over the vehicle resulted in large values of rolling and yawing moments which were not in phase with the motion. The derivatives became quite large at angles of attack near the stall, where sensitivity of the flow to small motions became severe and large areas of stalled flow were in evidence.

WIND-TUNNEL MEASUREMENT TECHNIQUES FOR $\dot{\beta}$ DERIVATIVES

Accurate analysis of the dynamic stability and control characteristics of airplanes depends directly on accurate aerodynamic inputs for computing time histories of aircraft motions and the stability of these motions. Theoretical prediction methods for the dynamic derivatives at high angles of attack have not advanced to the level of sophistication currently reflected in such methods for low angles of attack. Most of the information pertaining to these dynamic derivatives has therefore been generated by specialized wind-tunnel test techniques.

Rotary Forced-Oscillation Technique

The most common wind-tunnel method in current use for obtaining dynamic stability derivatives is the rotary forced-oscillation technique illustrated in figure 2. In this technique, a wind-tunnel model is forced to oscillate in roll or yaw at predetermined constant values of frequency and amplitude. A detailed discussion of the test setup and instrumentation required for a typical forced-oscillation technique is given in references 7 and 8.

It should be noted that because of kinematic constraints produced by this type of test, the measured dynamic stability parameters are a combination of the dynamic stability derivatives. For example, forced-oscillation tests in yaw produce a parameter $C_{n_r} - C_{n_{\dot{\beta}}} \cos \alpha$ in body axes, or $\left(C_{n_r}\right)_S - \left(C_{n_{\dot{\beta}}}\right)_S$ in stability axes. Unfortunately, the combined derivatives cannot be separated or individually identified by using rotary forced-oscillation techniques.

Linear Forced-Oscillation Techniques

In addition to the rotary-type forced-oscillation technique, several devices have been employed to provide a linear sidewise oscillatory motion for the measurement of the $\dot{\beta}$ derivatives. The linear-oscillation technique permits the measurement of "pure" $\dot{\beta}$ derivatives over a wide range of angle of attack. A sketch of the setup involved for such tests is given in figure 3, and detailed descriptions of the apparatus and instrumentation used may be found in references 2 and 4.

Curved- and Rolling-Flow Techniques

A unique wind tunnel was designed and constructed by the NACA at Langley in the early 1940's to permit the measurement of derivatives due to "pure" angular rates. This tunnel, known as the Langley stability tunnel, was acquired by the Virginia Polytechnic Institute in 1958, and is currently in operation at that institute. The wind tunnel functions in a conventional manner for the measurement of static stability and control derivatives; however, it also incorporates interchangeable circular and square test sections which permit specialized tests for the measurement of dynamic derivatives. The circular test section is equipped with a motor-driven rotor which imparts a helical motion to the airstream and thus subjects a stationary model to a flow field similar to that which exists about an airplane in rolling flight. In this manner it is possible to measure aerodynamic derivatives due to "pure" steady-state roll rates. A more detailed discussion of the rolling-flow technique is given in reference 9.

The square test section of the wind tunnel has a unique capability in that the vertical sidewalls are designed with sufficient flexibility so that they may be deflected into a curve, thus creating a curved airflow past the model. Jackscrews are positioned at regular intervals along each wall to allow the curvature to be set at predetermined values. In order to simulate flight in a curved path, it is necessary to redistribute the velocity profile in the radial direction in the tunnel. This need is accomplished by installing vertical wire screens in the flow upstream of the test section. These screens vary in mesh across the wind tunnel, with the most dense portion of the screens located nearer the center of curvature. A sketch showing a typical curved-flow test arrangement is shown in figure 4 and a

complete description of the tunnel and its operation is given in reference 10. With this test setup, it is possible to measure aerodynamic derivatives due to "pure" steady-state yaw rates.

Pure-Yawing-Oscillation Technique

In addition to the abovementioned techniques, an apparatus which superimposed both a yawing motion and a sidewise oscillatory motion was developed for the stability tunnel. With this apparatus, the resultant motion of the model was a pure yawing oscillation. A more detailed description of this test setup may be found in references 11 and 12.

By using results obtained from the pure-yawing, rolling-flow, and rotary forced-oscillation tests, it is theoretically possible to add or subtract the magnitudes of the various test results and obtain values of the $\dot{\beta}$ derivatives.

ILLUSTRATION OF TYPICAL RESULTS

Isolated Wings

Several investigations have been conducted to determine the physical causes of the $\dot{\beta}$ derivatives. In particular, tests conducted on isolated wings have provided some insight in this area.

Static considerations.- Shown in figure 5 are an unswept wing, a 45° swept wing, and a 60° delta wing, which were investigated in reference 3. The static longitudinal characteristics of the wings are presented in figure 6(a). These data show that the unswept wing stalled at an angle of attack of about 16°, the swept wing stalled at an angle of attack of about 25°, but the delta wing was not stalled at the maximum angle of attack (30°) reached in the tests. The effective dihedral derivative C_{l_β} as determined over the sideslip-angle range of $\pm 10^{\circ}$ is presented in figure 6(b) for each of the wings. The data show that the unswept wing experienced a large increase in positive dihedral effect near the stall, whereas the swept and delta wings exhibited large unstable values of $\left(C_{l_\beta}\right)_s$ near the stall. These characteristics are typical results for unswept and swept wings and may be interpreted in a physical sense from the flow patterns indicated in figure 6(c). In addition, the mechanism which produces large $\dot{\beta}$ derivatives for isolated wings may be anticipated from these flow patterns.

As shown in figure 6(c), the swept and delta wings shed strong vortices at high angles of attack, whereas the unswept wing does not. When subjected to sideslip, the advancing wing panel for the swept and delta wings becomes stalled, and there results a complete loss of dihedral effect. For the unswept wing the leading panel does not experience stall, but rather the trailing panel stalls, and a large increase in dihedral effect occurs as a result.

8

The foregoing characteristics are indicators of flow conditions which give rise to large values of the $\dot{\beta}$ derivatives during dynamic motions.

Results of dynamic tests.- The basic phenomenon responsible for large $\dot{\beta}$ derivatives for swept and delta wings is the time lag required for the previously discussed vortex flows of these wings to follow the dynamic motions of the wing. This characteristic has been shown for a delta wing in reference 13. In a static condition at high angles of attack and zero sideslip, the delta wing sheds two strong vortices which emanate from the apex of the wing and remain symmetrically displaced over the wing. Motion-picture photographs presented in reference 13 show that when the wing is subjected to oscillatory motions, the vortex flow field lags behind the model motion. Because of the flow lag the vortices are asymmetrically displaced at a time when the model is at zero sideslip. The resulting flow field thus creates a rolling moment which is due to the rate of change of sideslip. The foregoing discussion is a brief description of the mechanism wherein large values of $C_{l\dot{\beta}}$ are produced by swept and delta wings at high angles of attack.

Examples of the $\dot{\beta}$ derivatives measured for a 60° delta wing and a 45° swept wing are reported in reference 5 and presented in figure 7. The static longitudinal characteristics of the wings (tested in refs. 5, 11, 12, and 14) are presented in figure 8 and the static lateral-directional characteristics are presented in figure 9 for reference. Presented in figures 10 and 11 are representative data pertaining to the $\dot{\beta}$ derivatives for these wings.

Figure 10 gives a comparison of data for the delta wing obtained by the forced-oscillation-in-yaw technique (ref. 14) and the linear-oscillation technique (ref. 5) at two values of reduced frequency k. Also shown are data obtained from steady-state yawing tests (ref. 11) and the pure-yawing-oscillation tests (ref. 12). It should be noted that the results from the steady-state yawing tests and the pure-yawing-oscillation tests are in disagreement. The reason for the discrepancy is unknown; however, it should be noted that for either case the magnitudes of the $\dot{\beta}$ derivatives are larger than those of the derivatives due to pure yawing at high angles of attack, and the results of the forced-oscillation test technique provide a qualitative measure of these derivatives for isolated wings. The magnitudes of the derivatives are seen to be highly dependent on the value of k, with the larger values obtained for the lower value of k.

Similar results obtained for the 45° swept wing are presented in figure 11. The data show trends similar to those exhibited by the delta wing; however, agreement between results of the forced-oscillation and linear-oscillation techniques is not as good as the agreement obtained for the delta wing. In both cases it should be noted that the results indicate large values of $\left(C_{n\dot{\beta}}\right)_S$ and $\left(C_{l\dot{\beta}}\right)_S$; and it may be anticipated that in equations of motion, the use of forced-oscillation results as "pure" yawing derivatives would be completely erroneous for the configurations tested.

It might be expected that the magnitude of the $\dot{\beta}$ derivatives near the stall would be highly dependent on the amplitude and frequency of motion used in the forced-oscillation test technique. Although not presented herein, the results of several studies indicate that these derivatives may have large dependence on amplitude and frequency, and large nonlinear effects may be present at high angles of attack. In addition, because of the nature of the flow field associated with the $\dot{\beta}$ derivatives, Reynolds number effects may be significant.

The past research has also indicated that the $\dot{\beta}$ derivatives of unswept wings may be much smaller than those of swept wings at high angles of attack. For example, forced-oscillation test results (from ref. 3) for the unswept, the 45° swept, and the 60° delta wings of figure 5 are presented in figure 12 for two values of k. These data show that the magnitudes of $\left(C_{n_r}\right)_s - \left(C_{n_{\dot{\beta}}}\right)_s$ and $\left(C_{l_r}\right)_s - \left(C_{l_{\dot{\beta}}}\right)_s$ are much smaller for the unswept wing at high angles of attack. This result serves to emphasize the importance of wing sweep in the formation of $\dot{\beta}$ derivatives at high values of angle of attack.

Contribution of Vertical Tail

The second major contributor to the $\dot{\beta}$ derivatives at high angles of attack is the vertical tail. This contribution is a result of the lag of sidewash at the vertical-tail location. The lag of the sidewash, and its effect on the damping in yaw of the tail, is analogous to the lag of downwash and its effect on the damping in pitch of a horizontal tail, which was first discussed by Cowley and Glauert in reference 15. The lag of downwash was treated in the past as an additional angle of attack of the horizontal tail which was due to the time required for the wing disturbance to travel the distance between the wing and the horizontal tail. The case for the lag of sidewash at the vertical tail follows from the same physical mechanism, but the characteristic length involved is not as well defined.

Typical results of forced-oscillation-in-yaw tests for fighter configurations at high angles of attack indicate that the vertical tail may add considerable damping at high angles of attack, even though the tail may make no significant contribution to static directional stability. For example, shown in figure 13(a) are results obtained during static wind-tunnel tests for a current fighter configuration which is subject to loss of directional stability at high angles of attack. The data show that the contribution of the vertical tail to $C_{n_{\beta}}$ was markedly reduced above $\alpha = 30^{\circ}$. This result is usually attributed to a combination of reduced dynamic pressure and adverse sidewash at the vertical-tail location. However, as shown in figure 13(b), the combination of derivatives measured during forced-oscillation-in-yaw tests shows an increased vertical-tail contribution at high angles of attack. As indicated previously, this result may be attributed to the vertical-tail contribution to $C_{n_{\dot{\beta}}}$, which is associated with a lag of the sidewash. Analytical and exper-

imental results for the vertical-tail contribution to $C_{n_{\dot{\beta}}}$ are discussed in a subsequent section "Prediction Methods for $\dot{\beta}$ Derivatives."

EFFECT OF $\dot{\beta}$ DERIVATIVES ON DYNAMIC LATERAL-DIRECTIONAL STABILITY CHARACTERISTICS

The results of reference 1 show that the inclusion or omission of the $\dot{\beta}$ derivatives in theoretical equations of motion can produce large differences in the calculated dynamic stability characteristics. In particular, reference 1 shows that when data obtained from forced-oscillation tests — which represent a combination of derivatives — are used as a total value for the pure angular-rate derivatives and the $\dot{\beta}$ derivatives are assumed to equal zero, the results vary significantly from the results obtained when all pure derivatives are used. In addition, reference 16 has shown that the frequency effects of stability derivatives can cause considerable changes in predicted aircraft motion. In order to illustrate these results, calculations are made for a hypothetical delta-wing fighter configuration.

The mass and inertial properties used in the calculations are presented in table I and the aerodynamic characteristics for the configuration, obtained from references 4, 17, and 18, are presented in figure 14. It should be noted that the static lateral-directional characteristics of this configuration (fig. 14(b)) are typical of those exhibited by many current fighter configurations. In particular, the configuration exhibits a marked reduction in both directional stability and dihedral effect at high angles of attack. Experience has shown that these conditions usually result in a directional divergence, or "nose slice." The yawing and rolling derivatives (fig. 14(c)) were obtained by the rolling- and curved-flow test techniques previously discussed. The derivatives due to rate of change of sideslip (fig. 14(d)) were obtained from wind-tunnel tests in reference 4, and the magnitude of $C_{Y_{\dot{\beta}}}$ was assumed to be zero for the calculations. The dynamic lateral-directional stability characteristics were calculated by means of classical three-degree-of-freedom linearized equations for the configuration in trimmed flight at angles of attack of 20° and 28° at an assumed altitude of 7620 m (25 000 ft). The condition of $\alpha = 20^O$ represents a case for which the static and dynamic data indicate a stable configuration with relatively small values of the $\dot{\beta}$ derivatives. At $\alpha = 28^O$, the configuration exhibits static instability (negative value of C_{n_β}), a marked reduction in magnitude of C_{l_β}, and large values of the $\dot{\beta}$ derivatives.

The results of the calculations are presented in table II in terms of the time to halve amplitude $t_{1/2}$ and the nondimensional reduced frequency k of the various lateral-directional modes of motion. Positive values of $t_{1/2}$ represent damped (dynamically stable) modes of motion, whereas negative values represent undamped (dynamically

unstable) modes of motion. Case 1 represents the results of calculations in which the true values of the angular-rate derivatives were used and the $\dot{\beta}$ derivatives were omitted. Cases 2 to 4 represent the results of calculations in which the angular-rate derivatives were used, and the experimental values of the $\dot{\beta}$ derivatives based on data obtained for three different values of k were included. Cases 5 to 7 represent results for which the $\dot{\beta}$ derivatives were summed with the pure rate derivatives to form combinations similar to those obtained from conventional forced-oscillation tests. For these cases, the resulting sums were used as values for the rate derivatives and the $\dot{\beta}$ terms in the equations were set equal to zero.

In table II(a), the results obtained from the calculations for $\alpha = 20^\circ$ are presented. The results show that including the $\dot{\beta}$ derivatives (cases 2 to 4) increased the damping of the Dutch roll mode but had essentially no effect on the frequency of the Dutch roll mode or the damping of the roll and spiral modes. Combining the derivatives (cases 5 to 7) had little additional effect on the Dutch roll and roll modes; however, the spiral mode became unstable. The foregoing results, obtained for relatively small values of the $\dot{\beta}$ derivatives, indicate relatively minor effects caused by neglect or misuse of the $\dot{\beta}$ derivatives at low angles of attack. For $\alpha = 28^\circ$ (table II(b)), the data show pronounced differences caused by the relatively large $\dot{\beta}$ derivatives. Use of the angular-rate derivatives and omission of the $\dot{\beta}$ derivatives (case 1) resulted in a stable Dutch roll mode, a virtually neutral stable roll mode, and a very unstable spiral mode. However, when the $\dot{\beta}$ derivatives were included in the calculations (cases 2 to 4) the Dutch roll mode ceased to exist, and two additional aperiodic modes were formed. In addition, it is seen that the magnitude of the $\dot{\beta}$ derivatives used in the calculations has an effect on the computed values of the time to halve amplitude of the spiral and aperiodic modes. When the angular-rate and $\dot{\beta}$ derivatives were used in combination (cases 5 to 7), the damping of the entire system was redistributed, resulting in highly stable spiral and roll modes and a highly unstable Dutch roll mode. The foregoing results illustrate that in equations of motion, the conventional use of the rotary forced-oscillation data to represent derivatives due to pure angular rates is erroneous at high angles of attack, where the $\dot{\beta}$ derivatives are of significant magnitude.

In addition to having effects on dynamic stability, it would be expected that the $\dot{\beta}$ derivatives would also have a large effect on the design of control systems for flight conditions at high angles of attack and on related analysis techniques. For example, a recent study (ref. 19) has shown that omission of the $\dot{\beta}$ derivatives may produce considerable errors in parameter-identification techniques.

PREDICTION METHODS FOR $\dot{\beta}$ DERIVATIVES

The previous discussion has emphasized the large effects caused by conventional use of forced-oscillation data in equations of motion at high angles of attack. Unfortunately,

no analytical estimation method currently exists for prediction of the $\dot{\beta}$ derivatives, and the subject has received little attention in the literature. At the very least, a method is required to permit a realistic qualitative separation of the combined derivatives measured in conventional forced-oscillation tests. Such methods should consider the contributions of both the vertical tail and the wing to the $\dot{\beta}$ derivatives.

Vertical-Tail Contribution

Oscillating-airfoil theory.- Expressions for the lift and pitching moment arising from the unsteady circulation about a two-dimensional airfoil subjected to small sinusoidal oscillations were developed in reference 20. This analysis was extended to include the case of finite-span wings in reference 21 and applied to the case of an oscillating vertical tail in references 22 and 23. From the methods presented in references 22 and 23, the following expression for $\left(\Delta C_{n\dot{\beta}}\right)_V$ is developed:

$$\left(\Delta C_{n\dot{\beta}}\right)_V = -\frac{\pi}{2}\left(\frac{\bar{c}_v}{b}\right)^2 \frac{S_v}{S}\left(\frac{J}{k_v} + a + \frac{2aG}{k_v}\right) \tag{1}$$

where the unsteady circulation functions J and G are tabulated in reference 23 as a function of the aspect ratio and reduced-frequency parameter k_v of the vertical tail. Although the oscillating-airfoil theory is frequency dependent, its application to the present subject is extremely limited because it does not consider sidewash or separated-flow effects.

Lag of sidewash.- The following expression for $\left(\Delta C_{n\dot{\beta}}\right)_V$ is developed in reference 24 and is based on the hypothesis that the sidewash at the vertical tail affects the yawing moment through a time lag τ, where $\tau = l_v/V$:

$$\left(\Delta C_{n\dot{\beta}}\right)_V = -2\left(\frac{l_v}{b}\right)^2 \left(\Delta C_{Y\beta}\right)_V \frac{\partial \sigma}{\partial \beta} \tag{2}$$

(The negative sign has been introduced for consistency with the present notation for sidewash.) Essentially, this development assumed that the sidewash originates at the center of gravity of the configuration and requires a finite time for the flow field to impinge on the vertical tail. For a simple fuselage—vertical-tail model, with auxiliary fins placed at the center of gravity to generate sidewash, reference 24 shows that equation (2) yields results which correlate fairly well with experimental data.

Figure 15 shows the vertical-tail contribution to $C_{n\dot{\beta}}$ for the delta-wing fighter configuration of reference 4. The vertical-tail contribution was determined by subtracting

the experimental wing-fuselage data from the data for the complete configuration. Figure 15 also presents the vertical-tail contribution calculated with the oscillating-airfoil theory (eq. (1)) and the lag-of-the-sidewash theory (eq. (2)). In these calculations, the geometric characteristics were obtained from table I, and the unsteady circulation functions were obtained from reference 23; the increment $\left(\Delta C_{Y_\beta}\right)_V$ due to the vertical tail and the sidewash parameter $\partial\sigma/\partial\beta$ were obtained from reference 17.

From figure 15 it is seen that both the theories are completely inadequate for predicting the vertical-tail contribution to $C_{n_{\dot{\beta}}}$. The lack of correlation of the oscillating-airfoil theory is probably due to the neglect of the sidewash generated by the wings; the lack of correlation of the lag-of-the-sidewash theory is probably due to the fact that the sidewash at the vertical tail is not necessarily generated at the center of gravity, as was assumed in the development of that theory.

Wing Contribution

As discussed previously, reference 13 has shown that under oscillatory conditions the flow field of a 60° delta wing lags behind the model motions. This lag has been investigated in detail (see ref. 3) by means of oscillograph traces of the output of the yawing-moment channel of a strain-gage balance. Additionally, reference 3 considers the discrepancy between the theoretical static lateral-directional stability derivatives C_{n_β} and C_{l_β} (see ref. 25) and those measured in both conventional static force tests and in forced-oscillation tests. On the basis of these considerations, reference 3 has shown that the large values of $\left(C_{n_r}\right)_s - \left(C_{n_{\dot{\beta}}}\right)_s$ measured for delta wings at high angles of attack can be attributed to an incremental yawing moment which is produced by separated flow and which lags the motion by a roughly constant time interval. In addition, the increase in the magnitude of $\left(C_{n_r}\right)_s - \left(C_{n_{\dot{\beta}}}\right)_s$ with increasing angle of attack is not caused by an increase in the time lag and is therefore probably attributable solely to the increased strength of the vortex flow and separation at the higher angles of attack. This result has led to the development of the following expression for $C_{n_{\dot{\beta}}}$ (see ref. 3):

$$C_{n_{\dot{\beta}}} = \left[\left(C_{n_\beta}\right)_{theo} - \left(C_{n_\beta}\right)_{exp}\right]\frac{\sin\phi_n}{k} \tag{3}$$

where ϕ_n is the phase angle associated with separation effects.

Since equation (3) is presented in reference 3 without a detailed development, it is derived in the appendix. A similar expression for $C_{l_{\dot{\beta}}}$ is obtained:

14

$$C_{l_{\dot\beta}} = \left[\left(C_{l_\beta}\right)_{\text{theo}} - \left(C_{l_\beta}\right)_{\text{exp}}\right] \frac{\sin \phi_l}{k} \tag{4}$$

where ϕ_l is the phase angle associated with separation effects. Additionally, since the values of ϕ_n and ϕ_l are obtained by examination of oscillograph traces in reference 3, expressions for ϕ_n and ϕ_l are developed in the appendix and presented below:

$$\phi_n = \cos^{-1}\left[\frac{\left(C_{n_\beta}\right)_{\text{theo}} - \left(C_{n_\beta}\right)_k}{\left(C_{n_\beta}\right)_{\text{theo}} - \left(C_{n_\beta}\right)_{\text{exp}}}\right] \tag{5}$$

and

$$\phi_l = \cos^{-1}\left[\frac{\left(C_{l_\beta}\right)_{\text{theo}} - \left(C_{l_\beta}\right)_k}{\left(C_{l_\beta}\right)_{\text{theo}} - \left(C_{l_\beta}\right)_{\text{exp}}}\right] \tag{6}$$

The use of the flow-field-lag theory has been shown in reference 3 to yield results which correlate well with experimental results of a 60° delta wing over the range of frequency considered.

As an illustration of the applicability of this technique to complete configurations, the twin-jet fighter airplane studied in references 7, 26, and 27 is considered. Figure 16 shows the variation of the lateral-directional stability derivatives C_{n_β} and C_{l_β} with angle of attack. These data were obtained in reference 7 from conventional static force tests and from the in-phase data obtained for forced-oscillation-in-yaw tests (assuming that $k^2 C_{n_{\dot r}}$ and $k^2 C_{l_{\dot r}}$ are negligible) at a reduced frequency k of 0.156. Also presented in figure 16 are approximate theoretical values of C_{n_β} and C_{l_β}. These approximate values are developed by first obtaining the theoretical variation of $\left(C_{n_\beta}\right)_s$ and $\left(C_{l_\beta}\right)_s$ with lift coefficient for the wing-fuselage combination. (See ref. 25.) These values were then transferred to the body-axis system, and the experimentally determined increments to C_{n_β} and C_{l_β} due to the tail (evaluated at $\alpha = 0$) were added. The approximate theoretical values therefore represent reference values which would be obtained if separation effects were not present.

Figure 17 presents the calculated values of the acceleration-in-sideslip derivatives $C_{n_{\dot\beta}}$ and $C_{l_{\dot\beta}}$ obtained by applying the flow-field-lag theory (eqs. (3) to (6)) to the data of figure 16. Also presented in figure 17 are values of $C_{n_{\dot\beta}}$ and $C_{l_{\dot\beta}}$ obtained by subtraction of the data measured under conditions of pure yawing flow (ref. 27) from the data

measured with the forced-oscillation-in-yaw technique (ref. 7) at a reduced frequency of oscillation k of 0.156. Figure 17 shows that the flow-field-lag theory yields values of $C_{n_{\dot{\beta}}}$ and $C_{l_{\dot{\beta}}}$ which are in reasonable agreement with the data obtained from the combination of tests with yawing flow and forced oscillation in yaw. Although the foregoing method could be carried out for the present configuration only over a limited angle-of-attack range because equations (5) and (6) yield values of the cosine function greater than unity, it offers some promise for future development of predictive techniques.

CONCLUSIONS

From the present summary of experimental and theoretical results pertaining to the aerodynamic stability derivatives due to the rate of change of sideslip $\dot{\beta}$ the following conclusions are made:

1. The $\dot{\beta}$ derivatives $\left(C_{n_{\dot{\beta}}}\text{ and }C_{l_{\dot{\beta}}}\right)$ are large for swept- and delta-wing configurations at high angles of attack.

2. The physical flow phenomenon responsible for the $\dot{\beta}$ derivatives is associated with the establishment of leading-edge vortex sheets and flow separation on the wings at high angles of attack. Additionally, the large values of the $\dot{\beta}$ derivatives can be attributed to an increment in the aerodynamic moments produced by the separated flow, which lags the motion of the configuration.

3. The $\dot{\beta}$ derivatives are very dependent on the frequency of oscillation, with the larger values obtained for the lower frequency.

4. In equations of motion, the conventional use of the rotary forced-oscillation data to represent derivatives due to pure angular rates is erroneous at high angles of attack, where the $\dot{\beta}$ derivatives are of significant magnitude.

5. Both the oscillating-airfoil theory and the lag-of-the sidewash theory are inadequate for predicting the contribution of the vertical tail to $C_{n_{\dot{\beta}}}$.

6. The flow-field-lag theory, devised in NACA RM L55H05 and extended herein, is found to yield results which are in reasonable agreement with experimental data for a current twin-jet fighter aircraft.

Langley Research Center
National Aeronautics and Space Administration
Hampton, Va. 23665
June 17, 1975

APPENDIX

DEVELOPMENT OF EQUATIONS FOR $C_{n_{\dot\beta}}$ AND $C_{l_{\dot\beta}}$
BASED ON FLOW-FIELD-LAG THEORY (REF. 3)

The equations developed herein for $C_{n_{\dot\beta}}$ and $C_{l_{\dot\beta}}$ are based on the flow-field-lag theory (ref. 3) and are developed for the case of a pure sidewise oscillation. However, as will be discussed, they are applicable to the data obtained under conditions of forced oscillation in yaw.

For the pure-sidewise-oscillation technique, discussed in references 2 and 4, the yawing velocity and yawing acceleration are identically zero and the model undergoes continuous changes in sideslip and rate of change of sideslip. Therefore, the yawing-moment signal $C_n(t)$ may be expressed as

$$C_n(t) = \left(C_{n_\beta}\right)_k \beta(t) + \left(C_{n_{\dot\beta}}\right)_k \dot\beta(t) \tag{A1}$$

where, for harmonic oscillation (see ref. 4),

$$\beta(t) = \frac{y_0 \omega}{V} \cos \omega t \tag{A2}$$

Introducing the nondimensional frequency parameter $k = \omega b/2V$ yields

$$\beta(t) = \frac{2y_0}{b} k \cos \omega t \tag{A3}$$

Differentiating equation (A3) with respect to time and introducing the nondimensional form of $\dot\beta$ (that is, $\dot\beta = \dot\beta b/2V$) yields

$$\dot\beta = -\frac{2y_0}{b} k^2 \sin \omega t \tag{A4}$$

Substituting equations (A3) and (A4) into equation (A1) yields

$$C_n(t) = \left(C_{n_\beta}\right)_k \frac{2y_0}{b} k \cos \omega t - \left(C_{n_{\dot\beta}}\right)_k \frac{2y_0}{b} k^2 \sin \omega t \tag{A5}$$

Multiplying equation (A5) by $\cos \omega t$ and integrating over the period yields

$$\left(C_{n_\beta}\right)_k = \frac{b}{2y_0 k\pi} \int_0^{2\pi} C_n(t) \cos \omega t \, \omega \, dt \tag{A6}$$

APPENDIX

Similarly, multiplying equation (A5) by $\sin \omega t$ and integrating over the period yields

$$\left(C_{n_{\dot{\beta}}}\right)_k = - \frac{b}{2y_0 k^2 \pi} \int_0^{2\pi} C_n(t) \sin \omega t \, \omega \, dt \tag{A7}$$

Adding and subtracting a theoretical value of C_{n_β} (which would be obtained in the absence of flow-separation effects, see ref. 25) to equation (A6) yields

$$\left(C_{n_\beta}\right)_k = \left(C_{n_\beta}\right)_{theo} + \frac{b}{2y_0 k \pi} \int_0^{2\pi} C_n(t) \cos \omega t \, \omega \, dt - \left(C_{n_\beta}\right)_{theo} \tag{A8}$$

Since the $\dot{\beta}$ derivatives are assumed to arise from flow-separation effects, a theoretical yawing-moment coefficient may be developed in terms of the theoretical values of C_{n_β}. This theoretical yawing-moment coefficient assumes no flow separation and may be written as

$$\left[C_n(t)\right]_{theo} = \left(C_{n_\beta}\right)_{theo} \frac{2y_0 k}{b} \cos \omega t \tag{A9}$$

Multiplying equation (A9) by $\cos \omega t$ and integrating over the period yields

$$\left(C_{n_\beta}\right)_{theo} = \frac{b}{2y_0 k \pi} \int_0^{2\pi} \left[C_n(t)\right]_{theo} \cos \omega t \, \omega \, dt \tag{A10}$$

Substituting equation (A10) into equation (A8) yields

$$\left(C_{n_\beta}\right)_k = \left(C_{n_\beta}\right)_{theo} + \frac{b}{2y_0 k \pi} \int_0^{2\pi} \left\{C_n(t) - \left[C_n(t)\right]_{theo}\right\} \cos \omega t \, \omega \, dt \tag{A11}$$

Assuming

$$C_n(t) - \left[C_n(t)\right]_{theo} = \left[\left(C_{n_\beta}\right)_{exp} - \left(C_{n_\beta}\right)_{theo}\right] \frac{2y_0 k}{b} \cos \left(\omega t - \phi_n\right) \tag{A12}$$

where ϕ_n is the phase angle associated with separation effects, and substituting equation (A12) into (A11) yield, upon carrying out the integration,

$$\left(C_{n_\beta}\right)_k = \left(C_{n_\beta}\right)_{theo} + \left[\left(C_{n_\beta}\right)_{exp} - \left(C_{n_\beta}\right)_{theo}\right] \cos \phi_n \tag{A13}$$

18

APPENDIX

Rearranging equation (A13) and solving for ϕ_n yields

$$\phi_n = \cos^{-1}\left[\frac{\left(C_{n_\beta}\right)_{theo} - \left(C_{n_\beta}\right)_k}{\left(C_{n_\beta}\right)_{theo} - \left(C_{n_\beta}\right)_{exp}}\right] \tag{A14}$$

Substituting equation (A9) into equation (A12) and substituting the resulting expression for $C_n(t)$ into equation (A7) yield upon carrying out the integration,

$$C_{n_{\dot\beta}} = \left[\left(C_{n_\beta}\right)_{theo} - \left(C_{n_\beta}\right)_{exp}\right]\frac{\sin\phi_n}{k} \tag{A15}$$

where ϕ_n is given by equation (A14).

In a similar fashion it can be shown that

$$C_{l_{\dot\beta}} = \left[\left(C_{l_\beta}\right)_{theo} - \left(C_{l_\beta}\right)_{exp}\right]\frac{\sin\phi_l}{k} \tag{A16}$$

where ϕ_l is the phase angle associated with separation effects and is given by the expression

$$\phi_l = \cos^{-1}\left[\frac{\left(C_{l_\beta}\right)_{theo} - \left(C_{l_\beta}\right)_k}{\left(C_{l_\beta}\right)_{theo} - \left(C_{l_\beta}\right)_{exp}}\right] \tag{A17}$$

In the development of these equations, a sideward oscillatory motion was assumed; however, it should be noted that the expressions for $C_{n_{\dot\beta}}$ and $C_{l_{\dot\beta}}$ are functions of the in-phase derivatives $\left(C_{n_\beta}\right)_k$ and $\left(C_{l_\beta}\right)_k$. Although the in-phase data obtained from the forced-oscillation-in-yaw tests are a combination of derivatives, such as $C_{n_\beta} + k^2 C_{n_{\dot r}}$ and $C_{l_\beta} + k^2 C_{l_{\dot r}}$, experience has shown that the magnitudes of the $\dot r$ derivatives are usually negligible and the total in-phase components may be considered as pure derivatives $\left(C_{n_\beta}\right)_k$ and $\left(C_{l_\beta}\right)_k$. Therefore, the method in this appendix for evaluating $C_{n_{\dot\beta}}$ and $C_{l_{\dot\beta}}$ is also applicable to the data obtained from the forced-oscillation-in-yaw technique. Additionally, it should be noted that there is no restriction as to the use of the stability or body system of axes.

REFERENCES

1. Campbell, John P.; and Woodling, Carroll H.: Calculated Effects of the Lateral Acceleration Derivatives on the Dynamic Lateral Stability of a Delta-Wing Airplane. NACA RM L54K26, 1955.

2. Riley, Donald R.; Bird, John D.; and Fisher, Lewis R.: Experimental Determination of the Aerodynamic Derivatives Arising From Acceleration in Sideslip for a Triangular, a Swept, and an Unswept Wing. NACA RM L55A07, 1955.

3. Campbell, John P.; Johnson, Joseph L., Jr.; and Hewes, Donald E.: Low-Speed Study of the Effects of Frequency on the Stability Derivatives of Wings Oscillating in Yaw With Particular Reference to High Angle-of-Attack Conditions. NACA RM L55H05, 1955.

4. Lichtenstein, Jacob H.; and Williams, James L.: Effect of Frequency of Sideslipping Motion on the Lateral Stability Derivatives of a Typical Delta-Wing Airplane. NACA RM L57F07, 1957.

5. Lichtenstein, Jacob H.; and Williams, James L.: Low-Speed Investigation of the Effects of Frequency and Amplitude of Oscillation in Sideslip on the Lateral Stability Derivatives of a 60° Delta Wing, a 45° Sweptback Wing, and an Unswept Wing. NASA TN D-896, 1961. (Supersedes NACA RM L58B26.)

6. McKinney, M. O.: NACA Research on VTOL and STOL Aeroplanes. Sixth Anglo-American Aeronautical Conference, (Folkstone), Joan Bradbrooke and V. A. Libbey, eds., Roy. Aeronaut. Soc., 1959, pp. 1-24; Discussion, pp. 24-38.

7. Grafton, Sue B.; and Libbey, Charles E.: Dynamic Stability Derivatives of a Twin-Jet Fighter Model for Angles of Attack From -10° to 110°. NASA TN D-6091, 1971.

8. Chambers, Joseph R.; and Grafton, Sue B.: Static and Dynamic Longitudinal Stability Derivatives of a Powered 1/9-Scale Model of a Tilt-Wing V/STOL Transport. NASA TN D-3591, 1966.

9. MacLachlan, Robert; and Letko, William: Correlation of Two Experimental Methods of Determining the Rolling Characteristics of Unswept Wings. NACA TN 1309, 1947.

10. Bird, John D.; Jaquet, Byron M.; and Cowan, John W.: Effect of Fuselage and Tail Surfaces on Low-Speed Yawing Characteristics of a Swept-Wing Model as Determined in Curved-Flow Test Section of Langley Stability Tunnel. NACA TN 2483, 1951. (Supersedes NACA RM L8G13.)

11. Queijo, M. J.; Fletcher, Herman S.; Marple, C. G.; and Hughes, F. M.: Preliminary Measurements of the Aerodynamic Yawing Derivatives of a Triangular, a Swept, and an Unswept Wing Performing Pure Yawing Oscillations, With a Description of the Instrumentation Employed. NACA RM L55L14, 1956.

12. Letko, William; and Fletcher, Herman S.: Effects of Frequency and Amplitude on the Yawing Derivatives of Triangular, Swept, and Unswept Wings and of a Triangular-Wing—Fuselage Combination With and Without a Triangular Tail Performing Sinusoidal Yawing Oscillations. NACA TN 4390, 1958.

13. Bird, John D.; and Riley, Donald R.: Some Experiments on Visualization of Flow Fields Behind Low-Aspect-Ratio Wings by Means of a Tuft Grid. NACA TN 2674, 1952.

14. Fisher, Lewis R.: Experimental Determination of Effects of Frequency and Amplitude on the Lateral Stability Derivatives for a Delta, a Swept, and an Unswept Wing Oscillating in Yaw. NACA Rep. 1357, 1958. (Supersedes NACA RM L56A19.)

15. Cowley, W. L.; and Glauert, H.: The Effect of the Lag of the Downwash on the Longitudinal Stability of an Aeroplane and on the Rotary Derivative M_q. R. & M. No. 718, British A.R.C., 1921.

16. Brown, Albert E.; and Schy, Albert A.: Analysis of the Dynamic Lateral Stability of a Delta-Wing Airplane With Frequency-Dependent Stability Derivatives. NASA TN D-113, 1959.

17. Goodman, Alex; and Thomas, David F., Jr.: Effects of Wing Position and Fuselage Size on the Low-Speed Static and Rolling Stability Characteristics of a Delta-Wing Model. NACA Rep. 1224, 1955. (Supersedes NACA TN 3063.)

18. Jaquet, Byron M.; and Fletcher, Herman S.: Experimental Steady-State Yawing Derivatives of a 60° Delta-Wing Model as Affected by Changes in Vertical Position of the Wing and in Ratio of Fuselage Diameter to Wing Span. NACA TN 3843, 1956.

19. Nguyen, Luat T.: Evaluation of Importance of Lateral Acceleration Derivatives in Extraction of Lateral-Directional Derivatives at High Angles of Attack. NASA TN D-7739, 1974.

20. Theodorsen, Theodore: General Theory of Aerodynamic Instability and the Mechanism of Flutter. NACA Rep. 496, 1935.

21. Biot, M. A.; and Boehnlein, C. T.: Aerodynamic Theory of the Oscillating Wing of Finite Span. GALCIT Rep. No. 5, Sept. 1942.

22. Bird, John D.; Fisher, Lewis R.; and Hubbard, Sadie M.: Some Effects of Frequency on the Contribution of a Vertical Tail to the Free Aerodynamic Damping of a Model Oscillating in Yaw. NACA Rep. 1130, 1953. (Supersedes NACA TN 2657.)

23. Fisher, Lewis R.: Some Effects of Aspect Ratio and Tail Length on the Contribution of a Vertical Tail to Unsteady Lateral Damping and Directional Stability of a Model Oscillating Continuously in Yaw. NACA TN 3121, 1954.

24. Fisher, Lewis R.; and Fletcher, Herman S.: Effect of Lag of Sidewash on the Vertical-Tail Contribution to Oscillatory Damping in Yaw of Airplane Models. NACA TN 3356, 1955.

25. Campbell, John P.; and McKinney, Marion O.: Summary of Methods for Calculating Dynamic Lateral Stability and Response and for Estimating Lateral Stability Derivatives. NACA Rep. 1098, 1952. (Supersedes NACA TN 2409.)

26. Chambers, Joseph R.; and Anglin, Ernie L.: Analysis of Lateral-Directional Stability Characteristics of a Twin-Jet Fighter Airplane at High Angles of Attack. NASA TN D-5361, 1969.

27. Coe, Paul L., Jr.; and Newsom, William A., Jr.: Wind-Tunnel Investigation To Determine the Low-Speed Yawing Stability Derivatives of a Twin-Jet Fighter Model at High Angles of Attack. NASA TN D-7721, 1974.

BIBLIOGRAPHY

Campbell, John P.; and Mathews, Ward O.: Experimental Determination of the Yawing Moment Due to Yawing Contributed by the Wing, Fuselage, and Vertical Tail of a Midwing Airplane Model. NACA WR L-387, 1943. (Formerly NACA ARR 3F28.)

Bennett, Charles V.; and Johnson, Joseph L.: Experimental Determination of the Damping in Roll and Aileron Rolling Effectiveness of Three Wings Having 2^O, 42°, and 62° Sweepback. NACA TN 1278, 1947.

Feigenbaum, David; and Goodman, Alex: Preliminary Investigation at Low Speeds of Swept Wings in Rolling Flow. NACA RM L7E09, 1947.

Hunton, Lynn W.; and Dew, Joseph K.: Measurements of the Damping in Roll of Large-Scale Swept-Forward and Swept-Back Wings. NACA RM A7D11, 1947.

Ribner, Herbert S.: The Stability Derivatives of Low-Aspect-Ratio Triangular Wings at Subsonic and Supersonic Speeds. NACA TN 1423, 1947.

Tosti, Louis P.: Low-Speed Static Stability and Damping-in-Roll Characteristics of Some Swept and Unswept Low-Aspect-Ratio Wings. NACA TN 1468, 1947.

Letko, William; and Cowan, John W.: Effect of Taper Ratio on Low-Speed Static and Yawing Stability Derivatives of 45° Sweptback Wings With Aspect Ratio of 2.61. NACA TN 1671, 1948.

Goodman, Alex; and Brewer, Jack D.: Investigation at Low Speeds of the Effect of Aspect Ratio and Sweep on Static and Yawing Stability Derivatives of Untapered Wings. NACA TN 1669, 1948.

Queijo, M. J.; and Jaquet, Byron M.: Investigation of Effects of Geometric Dihedral on Low-Speed Static Stability and Yawing Characteristics of an Untapered 45° Sweptback-Wing Model of Aspect Ratio 2.61. NACA TN 1668, 1948.

Letko, William; and Jaquet, Byron M.: Effect of Airfoil Profile of Symmetrical Sections on the Low-Speed Static-Stability and Yawing Derivatives of 45° Sweptback Wing Models of Aspect Ratio 2.61. NACA RM L8H10, 1948.

Jaquet, Byron M.; and Brewer, Jack D.: Low-Speed Static-Stability and Rolling Characteristics of Low-Aspect-Ratio Wings of Triangular and Modified Triangular Plan Forms. NACA RM L8L29, 1949.

Letko, William; and Brewer, Jack D.: Effect of Airfoil Profile of Symmetrical Sections on the Low-Speed Rolling Derivatives of 45° Sweptback-Wing Models of Aspect Ratio 2.61. NACA RM L8L31a, 1949.

Jaquet, Byron M.; and Brewer, Jack D.: Effects of Various Outboard and Central Fins on Low-Speed Static-Stability and Rolling Characteristics of a Triangular-Wing Model. NACA RM L9E18, 1949.

Letko, William; and Wolhart, Walter D.: Effect of Sweepback on the Low-Speed Static and Rolling Stability Derivatives of Thin Tapered Wings of Aspect Ratio 4. NACA RM L9F14, 1949.

Lockwood, Vernard E.: Damping-in-Roll Characteristics of a 42.7$^{\mathrm{o}}$ Sweptback Wing as Determined From a Wind-Tunnel Investigation of a Twisted Semispan Wing. NACA RM L9F15, 1949.

Campbell, John P.; and Goodman, Alex: A Semiempirical Method for Estimating the Rolling Moment Due to Yawing of Airplanes. NACA TN 1984, 1949.

Bird, John D.; and Jaquet, Byron M.: A Study of the Use of Experimental Stability Derivatives in the Calculation of the Lateral Disturbed Motions of a Swept-Wing Airplane and Comparison With Flight Results. NACA Rep. 1031, 1951. (Supersedes NACA TN 2018.)

Goodman, Alex; and Fisher, Lewis R.: Investigation at Low Speeds of the Effect of Aspect Ratio and Sweep on Rolling Stability Derivatives of Untapered Wings. NACA Rep. 968, 1950. (Supersedes NACA TN 1835.)

Letko, William; and Riley, Donald R.: Effect of an Unswept Wing on the Contribution of Unswept-Tail Configurations to the Low-Speed Static- and Rolling-Stability Derivatives of a Midwing Airplane Model. NACA TN 2175, 1950.

Fisher, Lewis R.; and Michael, William H., Jr.: An Investigation of the Effect of Vertical-Fin Location and Area on Low-Speed Lateral Stability Derivatives of a Semitailless Airplane Model. NACA RM L51A10, 1951.

Letko, William: Effect of Vertical-Tail Area and Length on the Yawing Stability Characteristics of a Model Having a 45$^{\mathrm{o}}$ Sweptback Wing. NACA TN 2358, 1951.

Brewer, Jack D.; and Fisher, Lewis R.: Effect of Taper Ratio on the Low-Speed Rolling Stability Derivatives of Swept and Unswept Wings of Aspect Ratio 2.61. NACA TN 2555, 1951. (Supersedes NACA RM L8H18.)

Wolhart, Walter D.: Influence of Wing and Fuselage on the Vertical-Tail Contribution to the Low-Speed Rolling Derivatives of Midwing Airplane Models With 45$^{\mathrm{o}}$ Sweptback Surfaces. NACA TN 2587, 1951.

Lichtenstein, Jacob H.: Effect of High-Lift Devices on the Low-Speed Static Lateral and Yawing Stability Characteristics of an Untapered 45$^{\mathrm{o}}$ Sweptback Wing. NACA TN 2689, 1952. (Supersedes NACA RM L8G20.)

Bird, John D.; Lichenstein, Jacob H.; and Jaquet, Byron M.: Investigation of the Influence of Fuselage and Tail Surfaces on Low-Speed Static Stability and Rolling Characteristics of a Swept-Wing Model. NACA TN 2741, 1952. (Supersedes NACA RM L7H15.)

24

Queijo, M. J.; and Wells, Evalyn G.: Wind-Tunnel Investigation of the Low-Speed Static and Rotary Stability Derivatives of a 0.13-Scale Model of the Douglas D-558-II Airplane in the Landing Configuration. NACA RM L52G07, 1952.

Williams, James L.: Measured and Estimated Lateral Static and Rotary Derivatives of a 1/12-Scale Model of a High-Speed Fighter Airplane With Unswept Wings. NACA RM L53K09, 1954.

Hewes, Donald E.: Low-Speed Measurement of Static Stability and Damping Derivatives of a 60° Delta-Wing Model for Angles of Attack of 0° to 90°. NACA RM L54G22a, 1954.

Johnson, Joseph L., Jr.: Low-Speed Measurements of Rolling and Yawing Stability Derivatives of a 60° Delta-Wing Model. NACA RM L54G27, 1954.

Beam, Benjamin H.; Reed, Verlin D.; and Lopez, Armando E.: Wind-Tunnel Measurements at Subsonic Speeds of the Static and Dynamic-Rotary Stability Derivatives of a Triangular-Wing Airplane Model Having a Triangular Vertical Tail. NACA RM A55A28, 1955.

Fisher, Lewis R.; Lichtenstein, Jacob H.; and Williams, Katherine D.: A Preliminary Investigation of the Effects of Frequency and Amplitude on the Rolling Derivatives of an Unswept-Wing Model Oscillating in Roll. NACA TN 3554, 1956.

Johnson, Joseph L., Jr.: Low-Speed Measurements of Static Stability, Damping in Yaw, and Damping in Roll of a Delta, a Swept, and an Unswept Wing for Angles of Attack From 0° to 90°. NACA RM L56B01, 1956.

Letko, William: Experimental Determination at Subsonic Speeds of the Oscillatory and Static Lateral Stability Derivatives of a Series of Delta Wings With Leading-Edge Sweep From 30° to 86.5°. NACA RM L57A30, 1957.

Fletcher, Herman S.: Low-Speed Experimental Determination of the Effects of Leading-Edge Radius and Profile Thickness on Static and Oscillatory Lateral Stability Derivatives for a Delta Wing With 60° of Leading-Edge Sweep. NACA TN 4341, 1958.

Paulson, John W.: Low-Speed Measurements of Oscillatory Lateral Stability Derivatives of a Model of a 60° Delta-Wing Bomber. NASA TM X-13, 1959.

Shanks, Robert E.: Effect of Wing Crank and Sweepback on the Low Subsonic Stability and Control Characteristics of a Model of a Hypersonic Boost-Glide Type Airplane. NASA TM X-181, 1960.

Fisher, Lewis R.: Experimental Determination of the Effects of Frequency and Amplitude of Oscillation on the Roll-Stability Derivatives for a 60° Delta-Wing Airplane Model. NASA TN D-232, 1960. (Supersedes NACA RM L57L17.)

Llewellyn, Charles P.; and Wolhart, Walter D.: Effect of Reynolds Number on the Lateral-Stability Derivatives at Low Speed of Sweptback- and Delta-Wing— Fuselage Combinations Oscillating in Yaw. NASA TN D-398, 1960.

Shanks, Robert E.; and Smith, Charles C., Jr.: Low-Speed Measurements of Static and Oscillatory Lateral Stability Derivatives of a 1/5-Scale Model of a Jet-Powered Vertical-Attitude VTOL Research Airplane. NASA TN D-433, 1960.

Ware, George M.; and Shanks, Robert E.: Investigation of the Low Subsonic Stability and Control Characteristics of a Model of a Hypersonic Boost-Glide Airplane Designed for High Lift-Drag Ratios at Low Speeds. NASA TM X-534, 1961.

Boisseau, Peter C.: Investigation of the Low-Subsonic Flight Characteristics of a Model of a Supersonic Airplane Configuration Having Tail Surfaces Outboard of the Wing Tips. NASA TM X-541, 1961.

Paulson, John W.; and Shanks, Robert E.: Investigation of the Low-Subsonic Stability and Control Characteristics of a Free-Flying Model of a Thick 70° Delta Reentry Con- figuration. NASA TN D-913, 1961.

Fletcher, LeRoy S.: Dynamic Rotary Stability Derivatives of a Delta-Winged Configura- tion With a Canard Control and Nacelles at Mach Numbers From 0.25 to 3.50. NASA TM X-781, 1963.

Shanks, Robert E.: Low-Subsonic Measurements of Static and Dynamic Stability Deriva- tives of Six Flat-Plate Wings Having Leading-Edge Sweep Angles of 70° to 84°. NASA TN D-1822, 1963.

Freeman, Delma C., Jr.: Low-Speed Measurements of Static and Oscillatory Lateral Stability Derivatives of a Supersonic Transport Model With a Highly Swept Wing. NASA TM X-1250, 1966.

Wiley, Harleth G.; and Brower, Margaret L.: Damping and Oscillatory Stability in Pitch and Yaw for a Model of an HL-10 Configuration at Mach Numbers From 0.20 to 1.00. NASA TM X-1467, 1967.

Freeman, Delma C.; Grafton, Sue B.; and D'Amato, Richard: Static and Dynamic Stabil- ity Derivatives of a Model of a Jet Transport Equipped With External-Flow Jet- Augmented Flaps. NASA TN D-5408, 1969.

Anglin, Ernie L.; and Grafton, Sue B.: Results of Static and Dynamic Force Tests of a 1/11-Scale Model of the F-4 Airplane and Their Applicability to Theoretical Spin Analysis – COORD NO. N-AM-147. NASA TM SX-2124, Naval Air Systems Com- mand, 1970.

Grafton, Sue B.; Parlett, Lysle P.; and Smith, Charles C., Jr.: Dynamic Stability Derivatives of a Jet Transport Configuration With High Thrust-Weight Ratio and an Externally Blown Jet Flap. NASA TN D-6440, 1971.

Grafton, Sue B.; and Anglin, Ernie L.: Dynamic Stability Derivatives at Angles of Attack From -5° to 90° for a Variable-Sweep Fighter Configuration With Twin Vertical Tails. NASA TN D-6909, 1972.

Grafton, Sue B.; Chambers, Joseph R.; and Coe, Paul L., Jr.: Wind-Tunnel Free-Flight Investigation of a Model of a Spin-Resistant Fighter Configuration. NASA TN D-7716, 1974.

TABLE I.- MASS AND GEOMETRIC CHARACTERISTICS OF THE DELTA-WING AIRPLANE

Mass, kg (slugs) 17 727 (1215)

Moments of inertia, kg-m^2 (slug-ft^2):

I_X 40 606 (29 950)

I_Z 229 859 (169 538)

I_{XZ} 7106 (5241)

Overall length, m (ft) 15.90 (52.16)

Wing:

Span, m (ft) 10.75 (35.26)

Area, m^2 (ft^2) 50.00 (538.30)

Mean aerodynamic chord, m (ft) 6.21 (20.38)

Aspect ratio 2.31

Taper ratio 0

Dihedral, deg 0

Incidence, deg 0

Leading-edge sweep, deg 60

Airfoil section . . . . NACA 65A003

Vertical tail:

Span, m (ft) 3.53 (11.59)

Area, m^2 (ft^2) 5.72 (61.59)

Root chord, m (ft) 3.24 (10.63)

Taper ratio 0

Leading-edge sweep, deg 42.5

Airfoil section . . . . NACA 65-006

Mean aerodynamic chord, m (ft) 2.16 (7.10)

Area ratio, S_v/S 0.115

Tail-length ratio, l_v/b 0.59

Aspect ratio 2.18

Tail length, m (ft) 6.33 (20.77)

TABLE II.- CALCULATED DYNAMIC STABILITY CHARACTERISTICS

(a) $\alpha = 20^{o}$

		Aerodynamic derivatives												Results					
														Dutch roll mode		Roll mode	Spiral mode	Aperiodic modes	
Case	k	C_{Y_β}	C_{n_β}	C_{l_β}	$C_{Y_{\dot\beta}}$	$C_{n_{\dot\beta}}$	$C_{l_{\dot\beta}}$	C_{Y_p}	C_{n_p}	C_{l_p}	C_{Y_r}	C_{n_r}	C_{l_r}	$t_{1/2}$, sec	k	$t_{1/2}$, sec	$t_{1/2}$, sec	$t_{1/2}$, sec	
	(a)																		
1	----	-0.510	0.135	-0.155	0	0	0	0.239	-0.062	-0.168	0.513	-0.332	0.023	11.99	0.086	1.79	16.03	---	---
2	0.066					-.130	-.357							4.35	.086	1.79	16.10	---	---
3	.109					-.239	-.306							5.63	.086	1.79	16.10	---	---
4	.132					-.280	-.258							6.97	.086	1.79	16.11	---	---
[b]5	.066					0	0		-.107	-.290		-.210	.358	4.42	.085	1.48	-19.63	---	---
[b]6	.109					0	0		-.144	-.273		-.107	.311	5.70	.086	1.46	-15.46	---	---
[b]7	.132					0	0		-.158	-.256		-.069	.265	7.02	.086	1.60	-15.49	---	---

[a] Reduced frequency at which $\dot\beta$ derivatives were measured.

[b] $\dot\beta$ derivatives combined with pure angular-rate derivatives.

(b) $\alpha = 28^{o}$

		Aerodynamic derivatives												Results					
														Dutch roll mode		Roll mode	Spiral mode	Aperiodic modes	
Case	k	C_{Y_β}	C_{n_β}	C_{l_β}	$C_{Y_{\dot\beta}}$	$C_{n_{\dot\beta}}$	$C_{l_{\dot\beta}}$	C_{Y_p}	C_{n_p}	C_{l_p}	C_{Y_r}	C_{n_r}	C_{l_r}	$t_{1/2}$, sec	k	$t_{1/2}$, sec	$t_{1/2}$, sec	$t_{1/2}$, sec	
	(a)																		
1	----	-0.195	-0.121	-0.015	0	0	0	0.155	-0.011	-0.214	0.400	-0.260	-0.171	1.27	0,014	51.14	-1.15	---	---
2	0.066					.452	-1.940							----	----	46.21	-2.85	1.72	0.34
3	.109					.387	-.998							----	----	48.52	-2.00	1.48	.54
4	.132					.336	-.858							----	----	48.88	-1.87	1.43	.60
[b]5	.066					0	0		.201	-1.125		-.659	1.542	-2.44	.019	.32	1.12	---	---
[b]6	.109					0	0		.171	-.683		-.602	.710	-2.36	.015	.52	1.05	---	---
[b]7	.132					0	0		.147	-.617		-.557	.586	-2.33	.013	.58	1.02	---	---

[a] Reduced frequency at which $\dot\beta$ derivatives were measured.

[b] $\dot\beta$ derivatives combined with pure angular-rate derivatives.
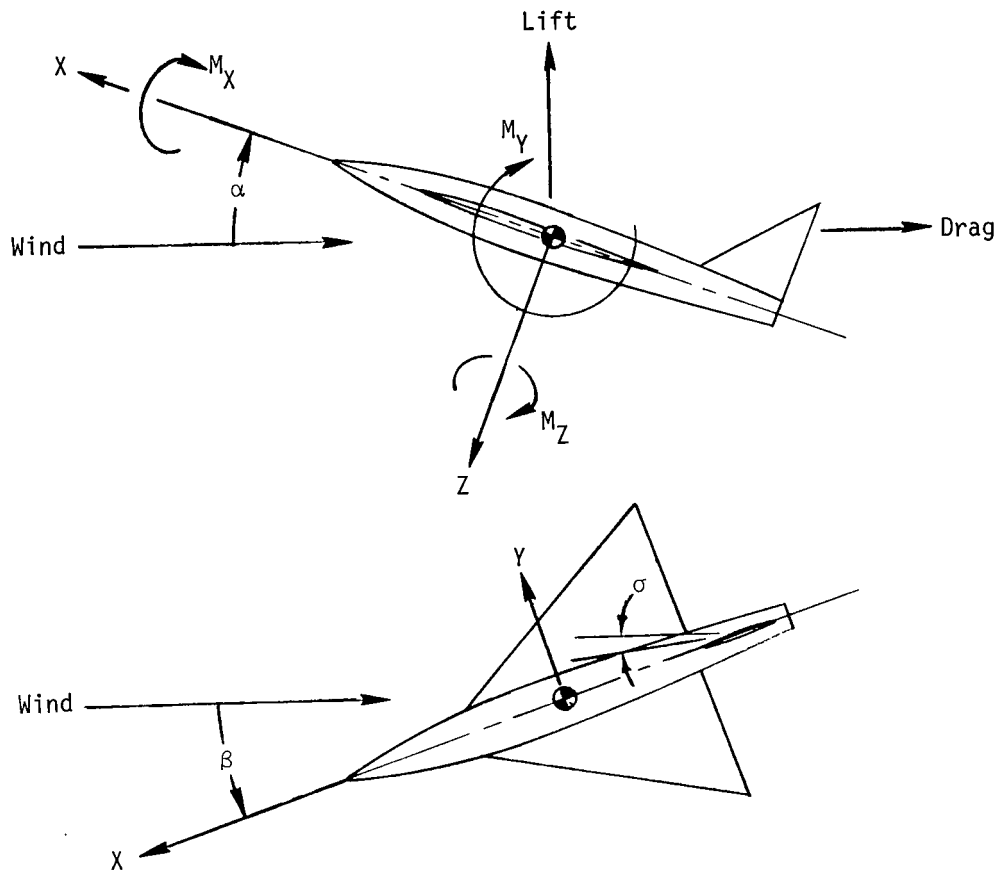
Figure 1.- Body system of axes.
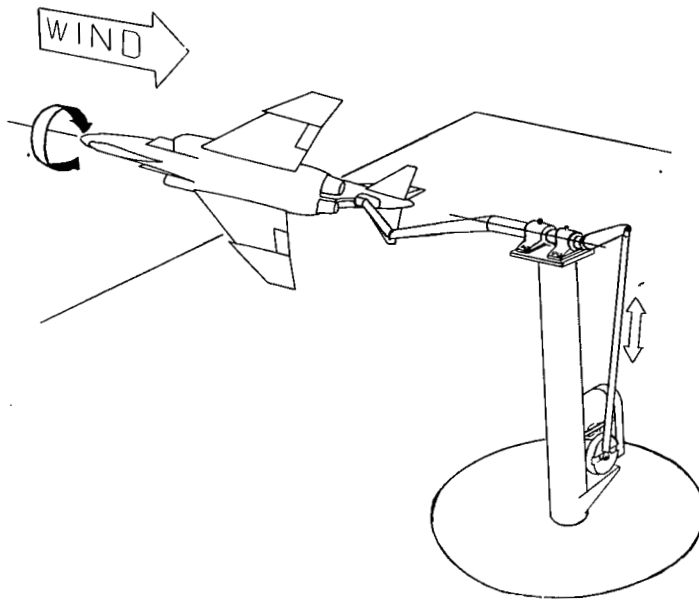
(a) Rolling setup.
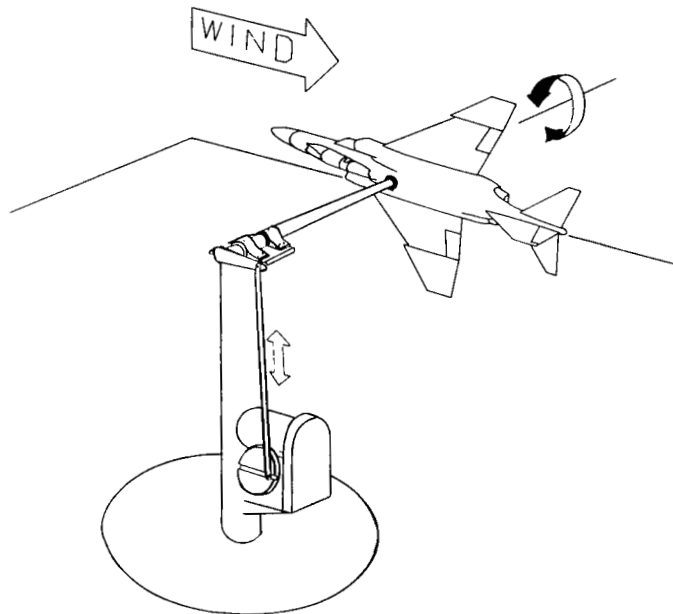
(b) Yawing setup.

Figure 2.- Sketch of test setup for rotary forced-oscillation tests.
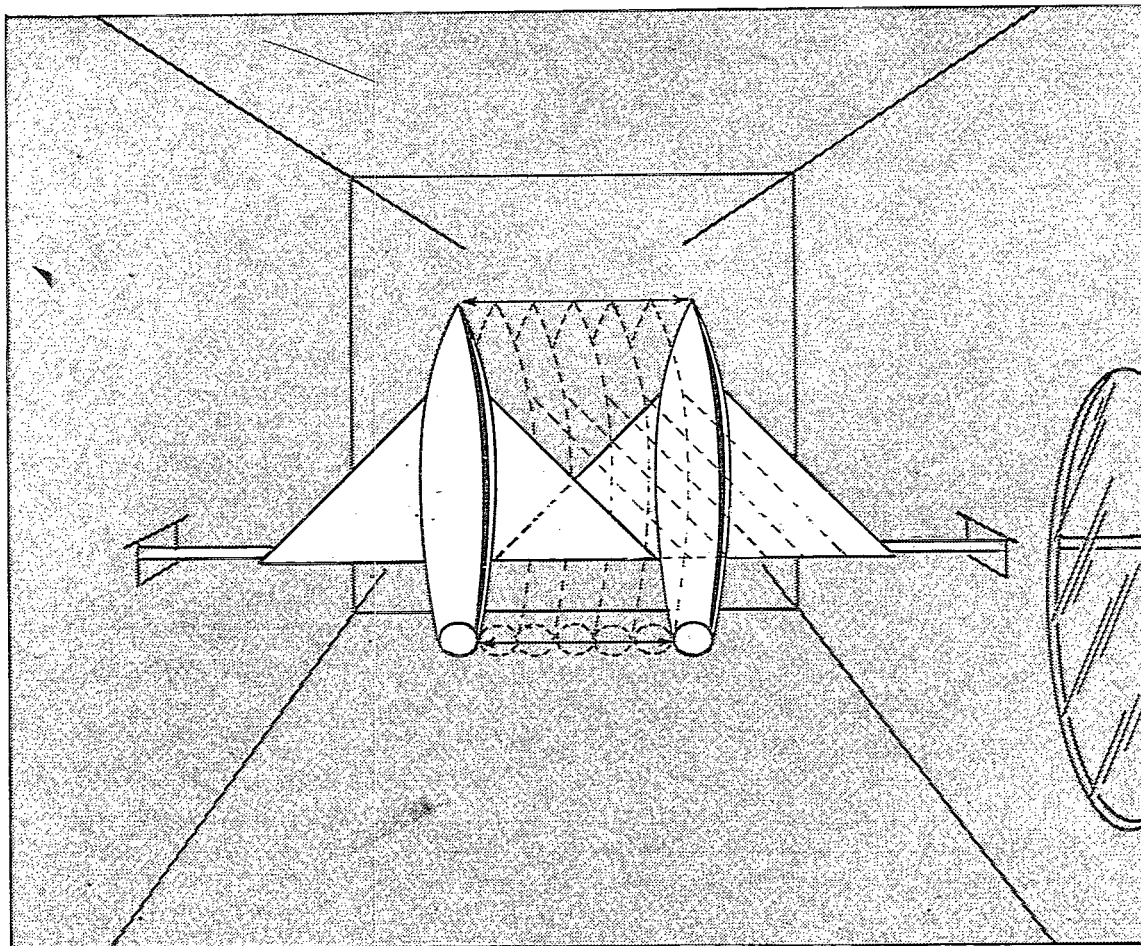
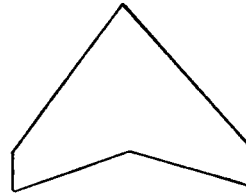Figure 3.- Sketch of test setup for linear sidewise oscillation test.
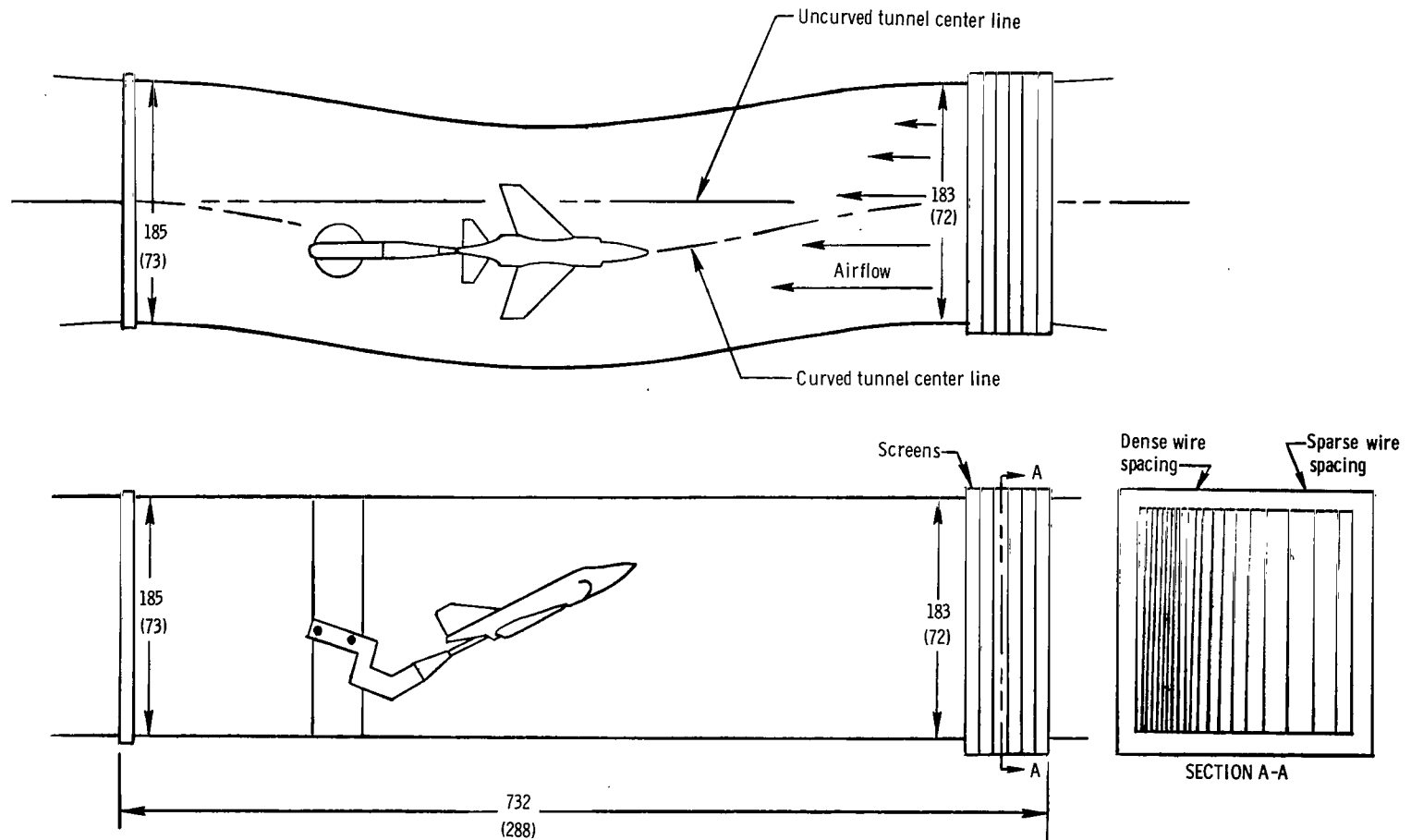
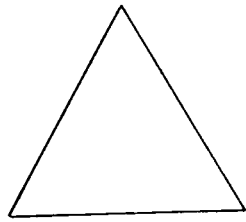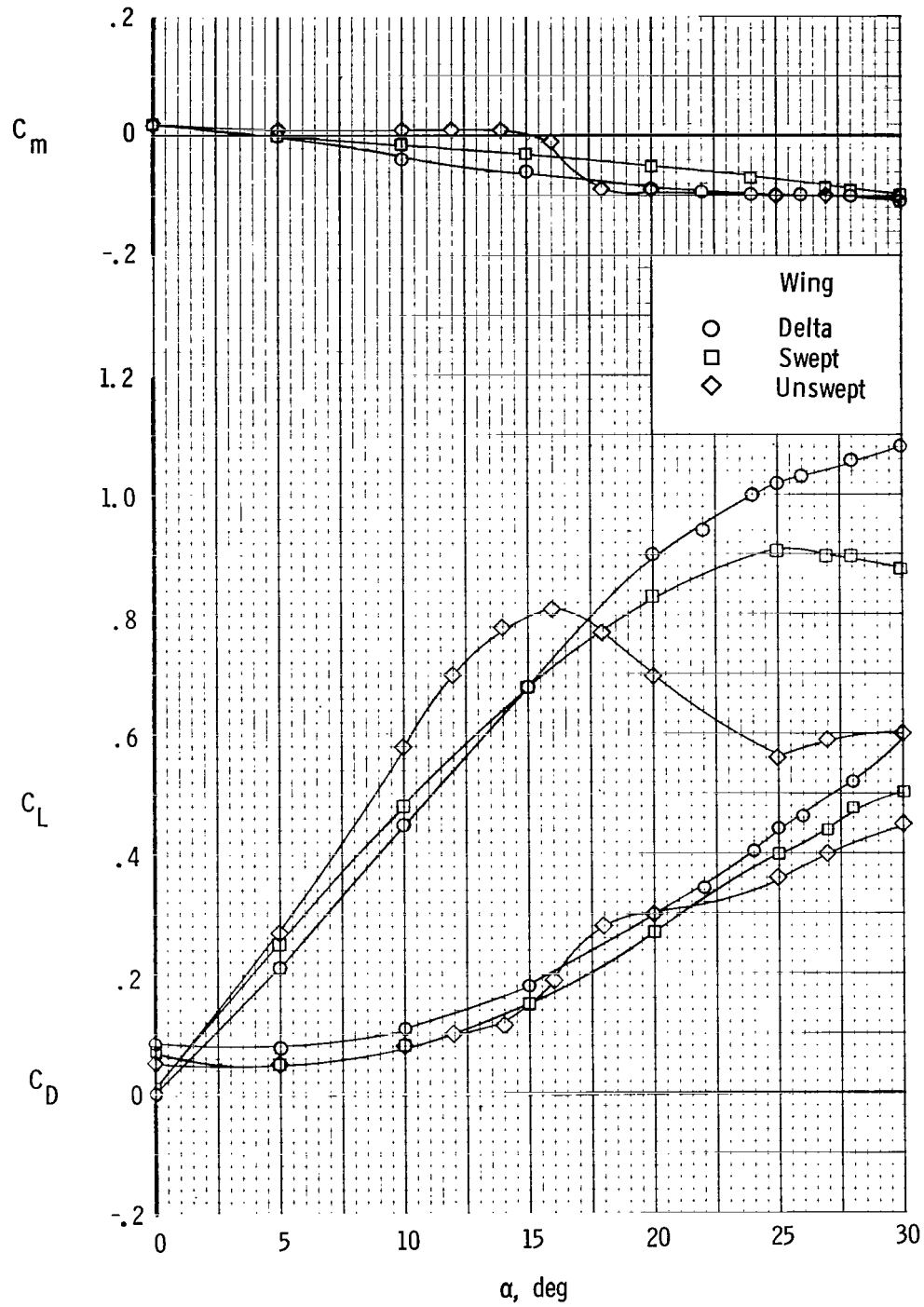Figure 4.- Diagram of curved-flow test section of wind tunnel. Dimensions are given in centimeters and parenthetically in inches.
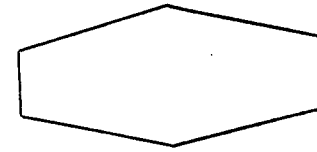
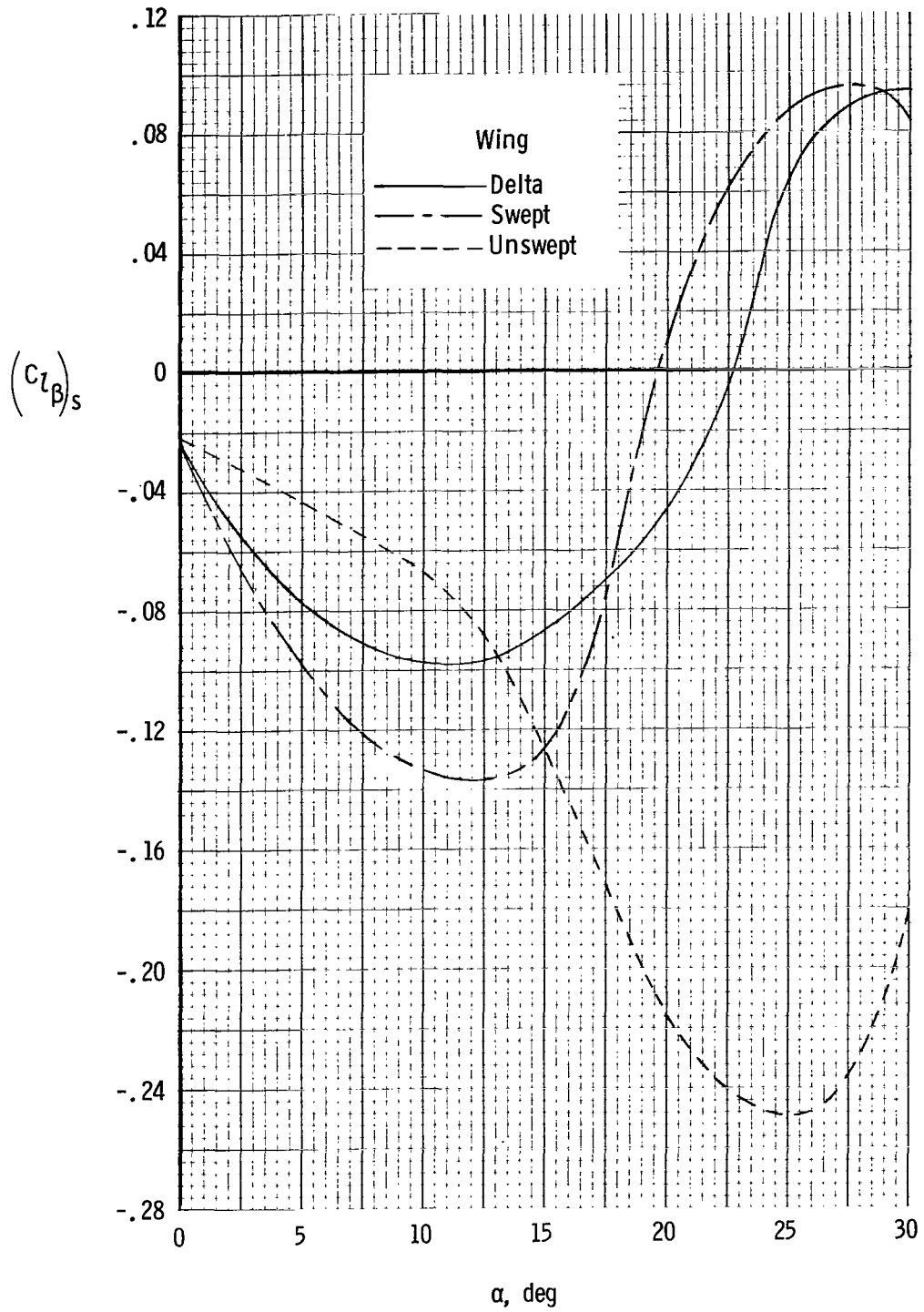|	Delta	Swept	Unswept
Type	Delta	Swept	Unswept
Sweep	$60°$(L.E.)	$45°(\overline{c}/4)$	$0°(\overline{c}/2)$
Aspect ratio	2.31	2.61	3.00
λ	0	0.25	0.50
Airfoil	NACA 65-006.5	NACA 0012	NACA 0012

Figure 5.- Sketch showing geometric characteristics of wings tested in reference 3.

(a) Static longitudinal characteristics.

Figure 6.- Variation of aerodynamic characteristics with angle of attack for three wings tested in reference 3.

(b) Effective dihedral derivative.

Figure 6.- Continued.

Type

Delta

Separated flow
Attached flow

Swept

Unswept

Low angles of attack   High angles of attack
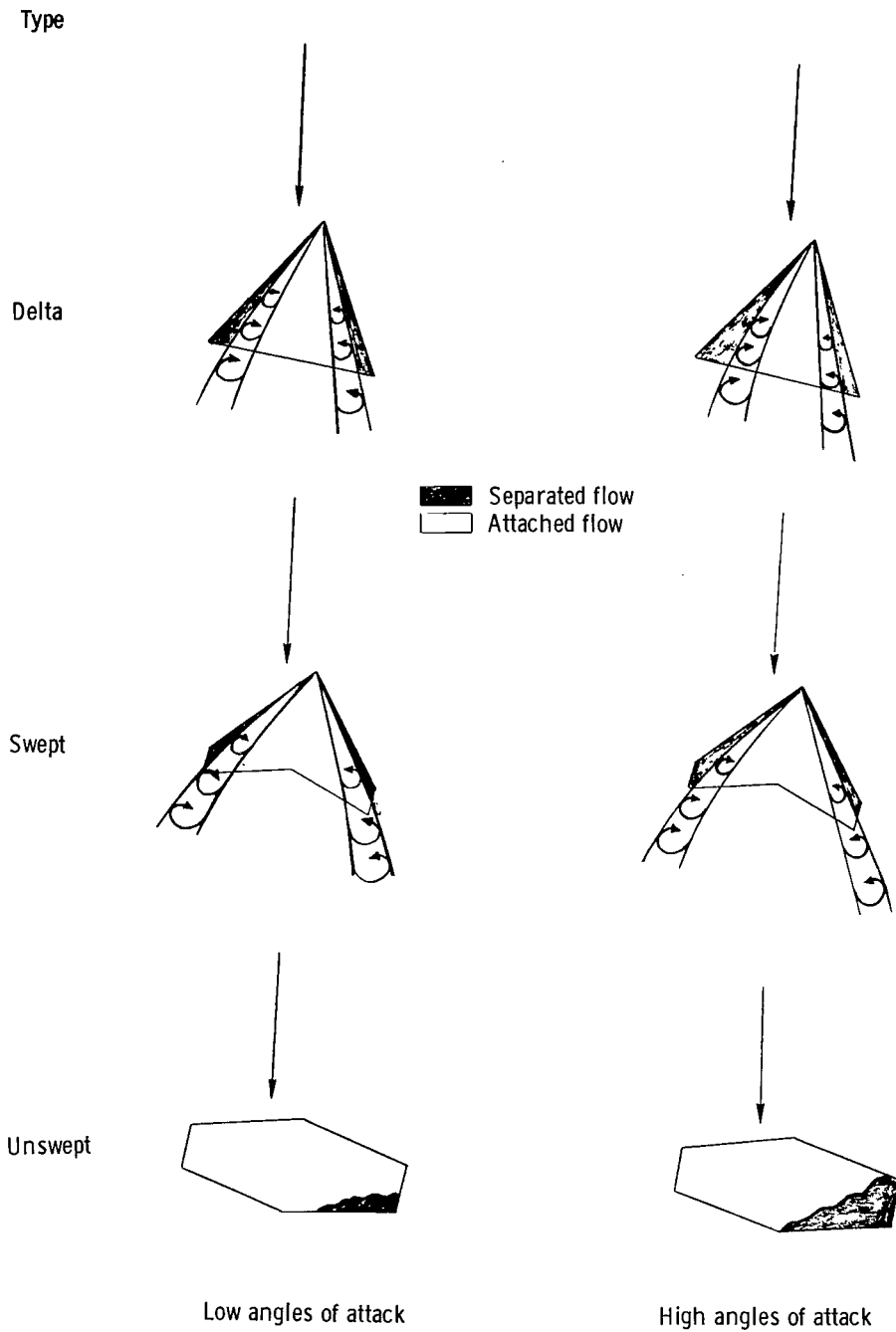
(c) Upper-surface flow characteristics in sideslip.

Figure 6.- Concluded.

(a) k = 0.066.

(b) k ≈ 0.218.
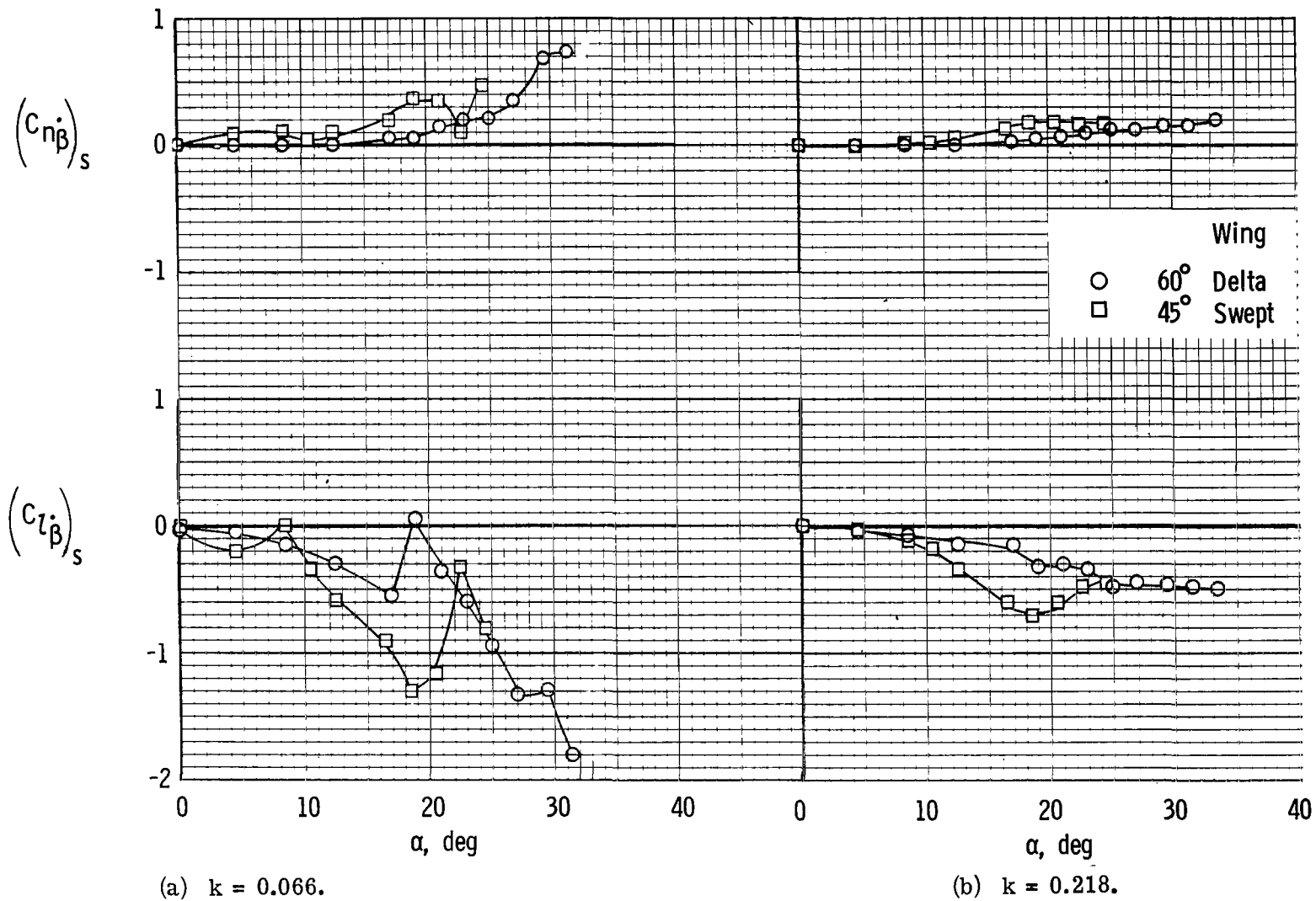
Figure 7.- Derivatives due to rate of change of sideslip for wings tested in reference 5.
Amplitude of oscillation, ±2°.
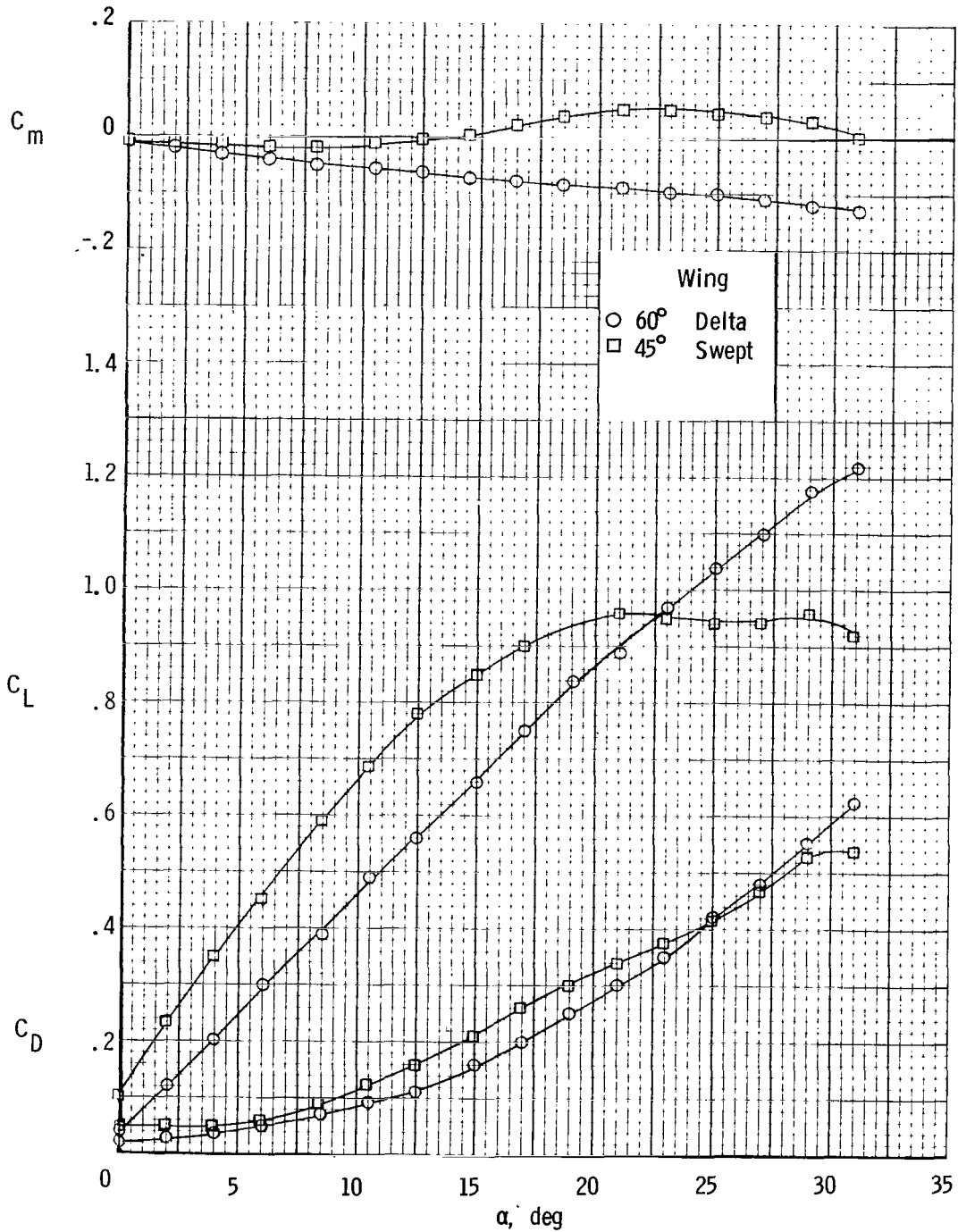
Figure 8.- Variation with angle of attack of static longitudinal characteristics of wings tested in references 5, 11, 12, and 14.
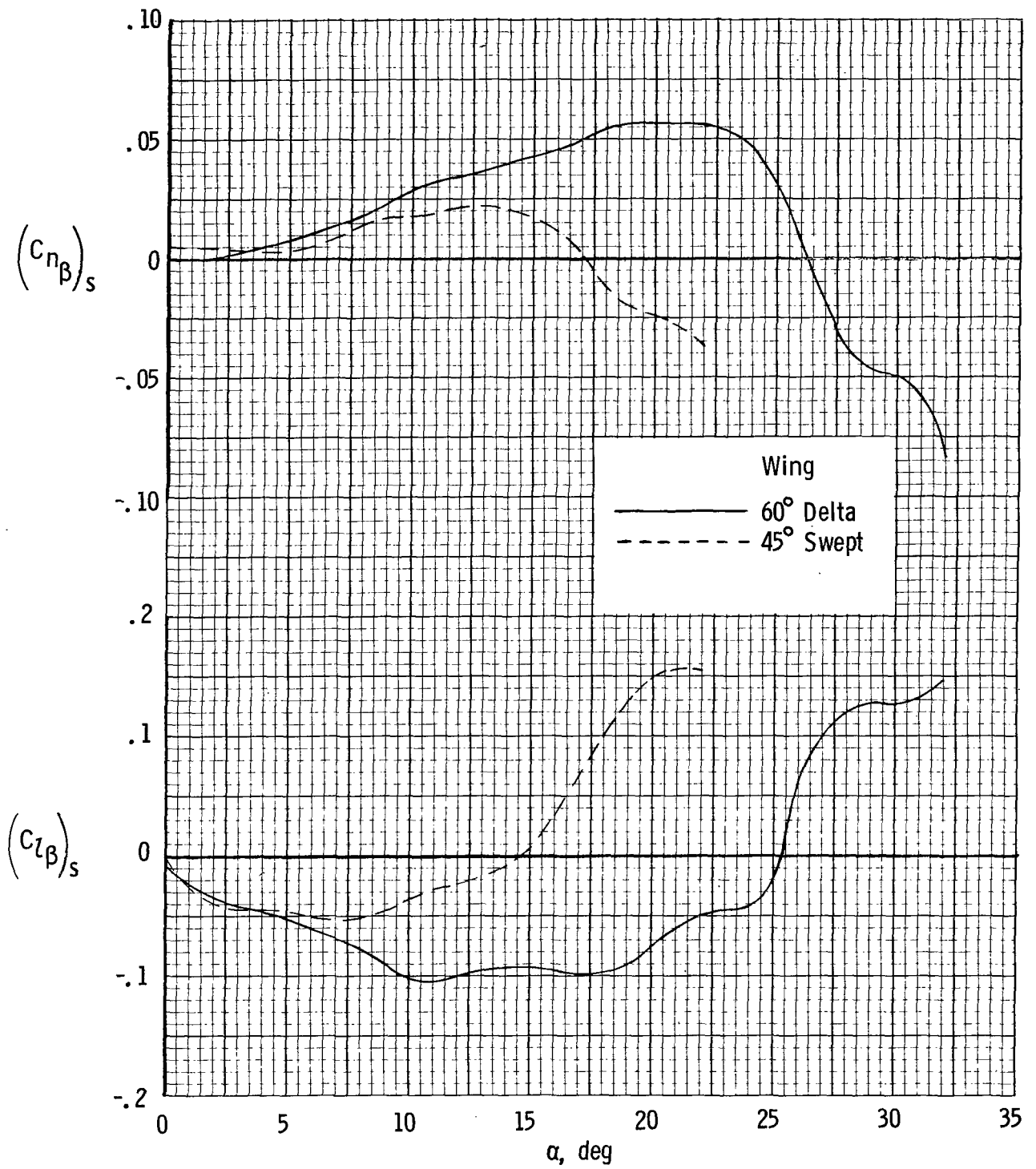
Figure 9.- Variation with angle of attack of static lateral-directional stability derivatives of wings tested in references 5, 11, 12, and 14.

(a) Low frequency.

(b) High frequency.
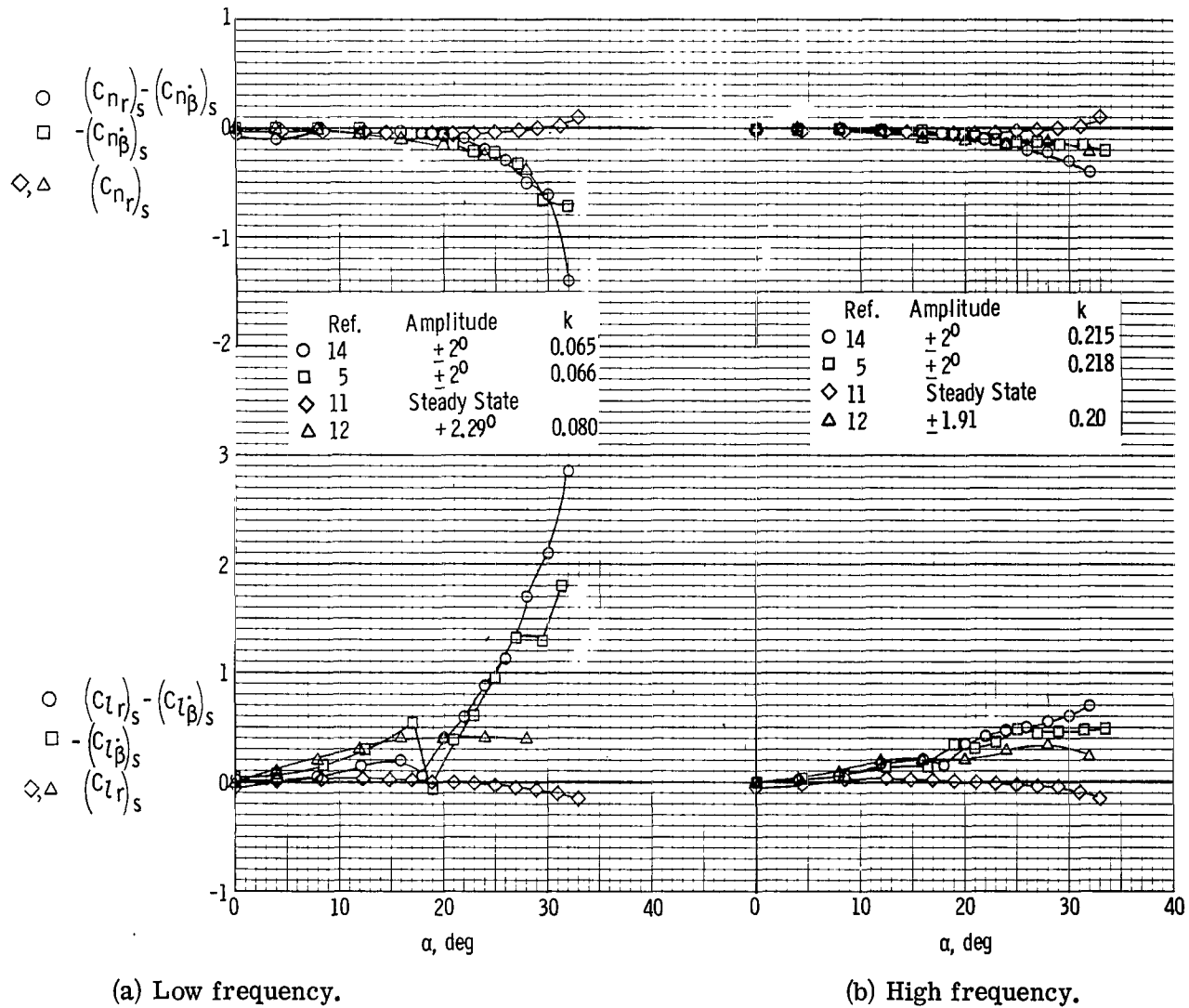
Figure 10.- Comparison of data obtained by various test techniques for 60° delta wing.

(a) Low frequency.　　　　　　　　(b) High frequency.
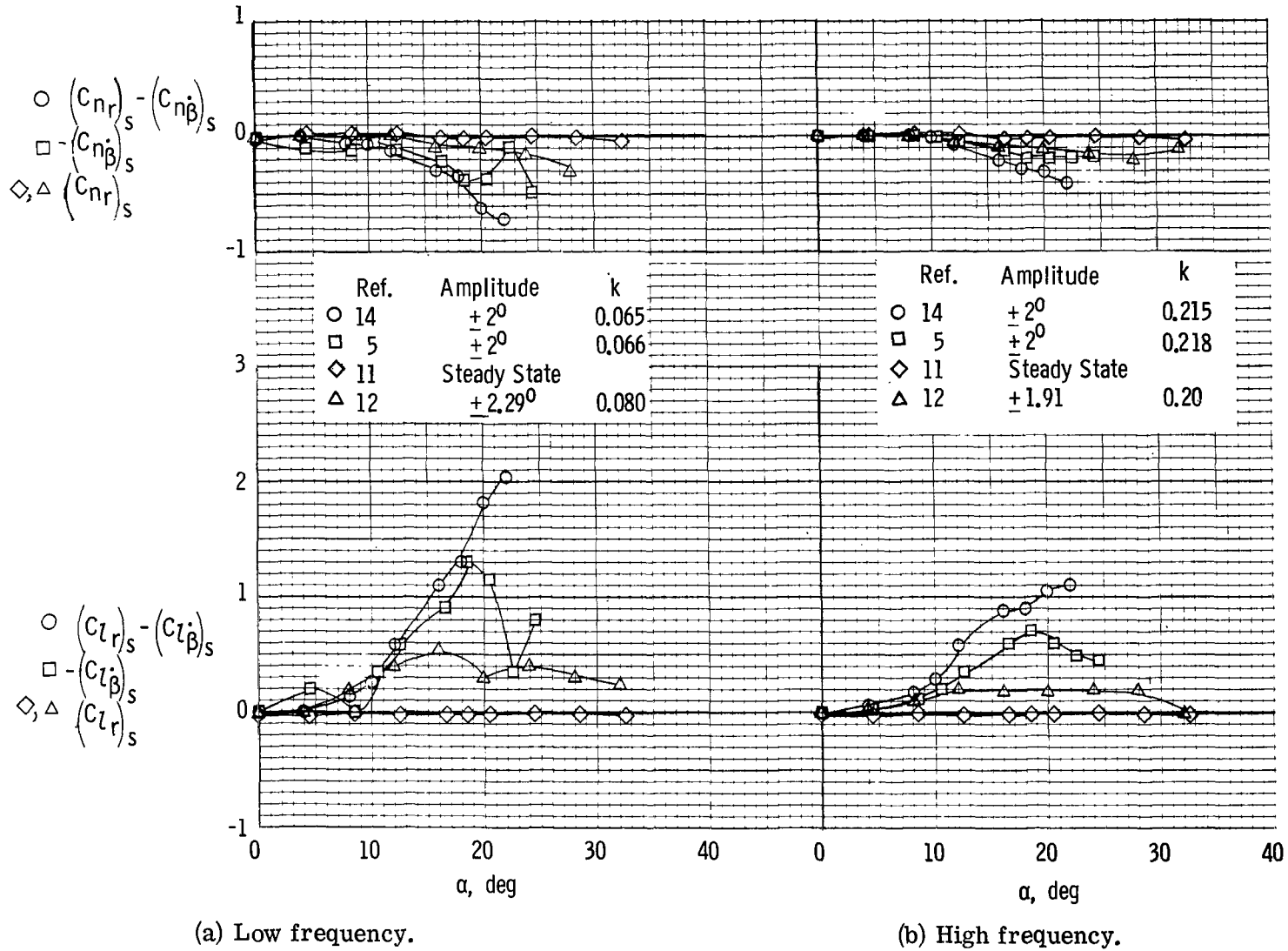
Figure 11.- Comparison of data obtained by various test techniques for 45° swept wing.
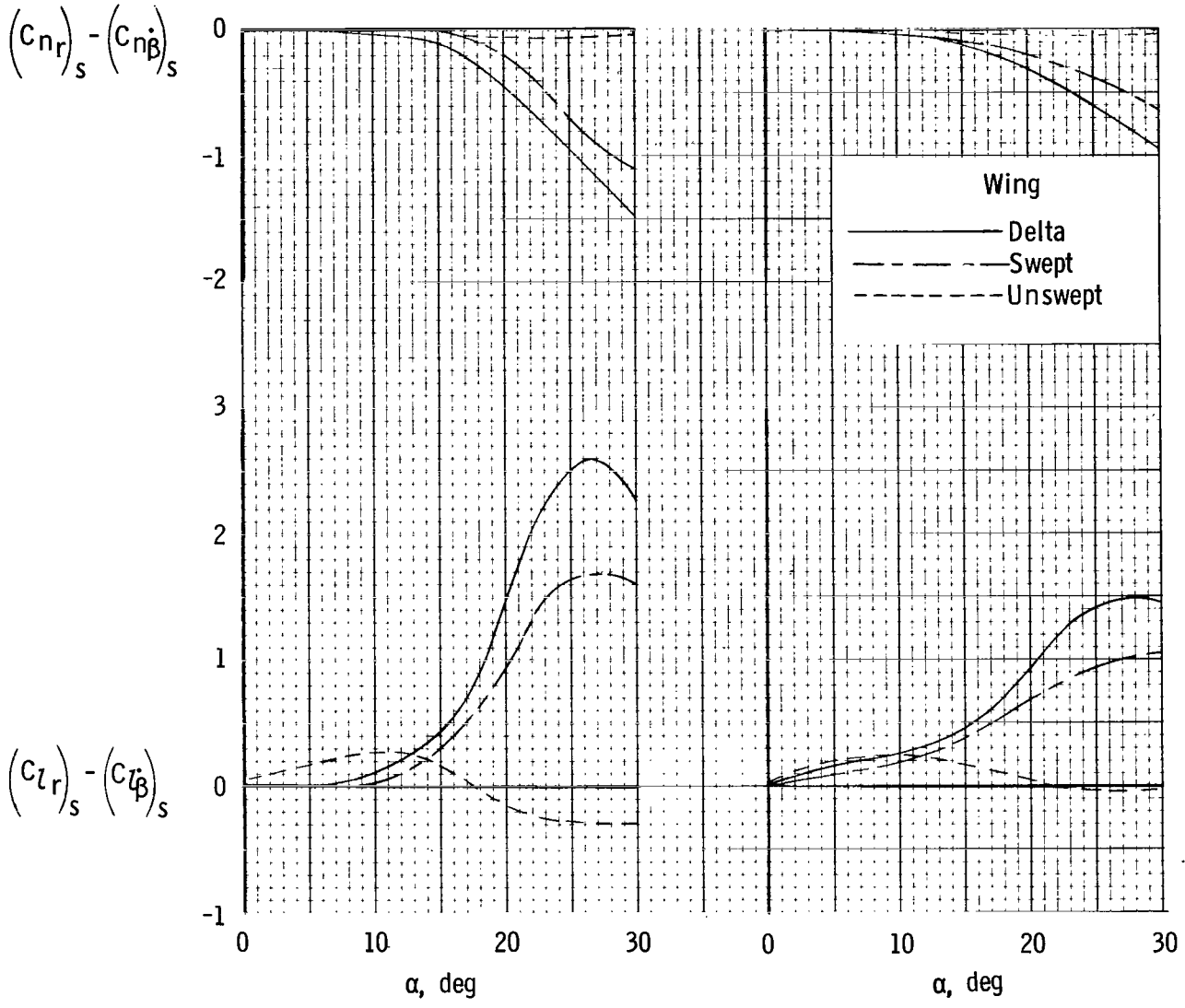
Figure 12.- Variation of $\left(C_{n_r}\right)_s - \left(C_{n_{\dot{\beta}}}\right)_s$ and $\left(C_{l_r}\right)_s - \left(C_{l_{\dot{\beta}}}\right)_s$ with angle of attack for wings tested in reference 3.
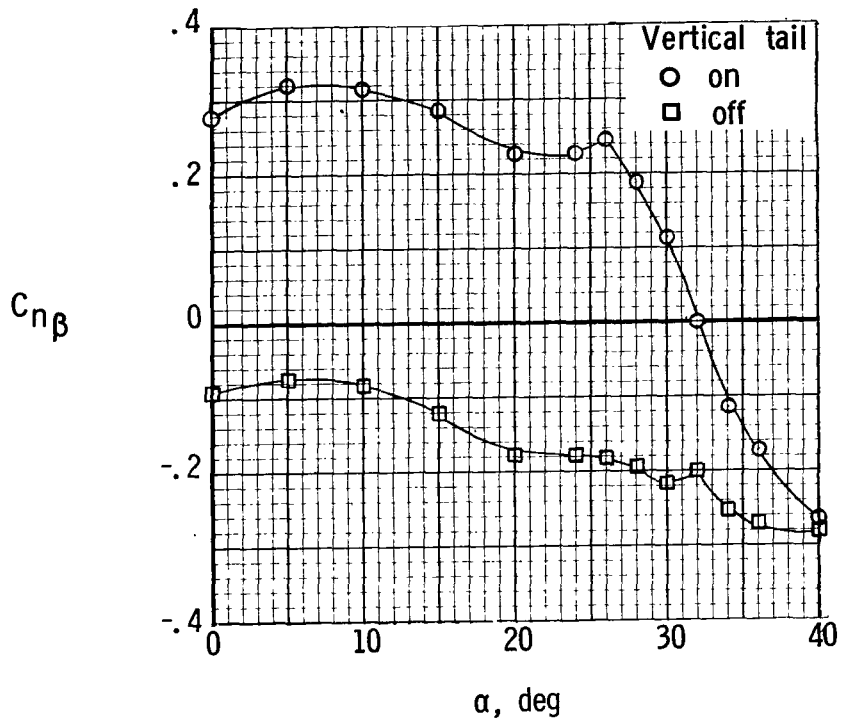
(a) Static directional stability derivative.
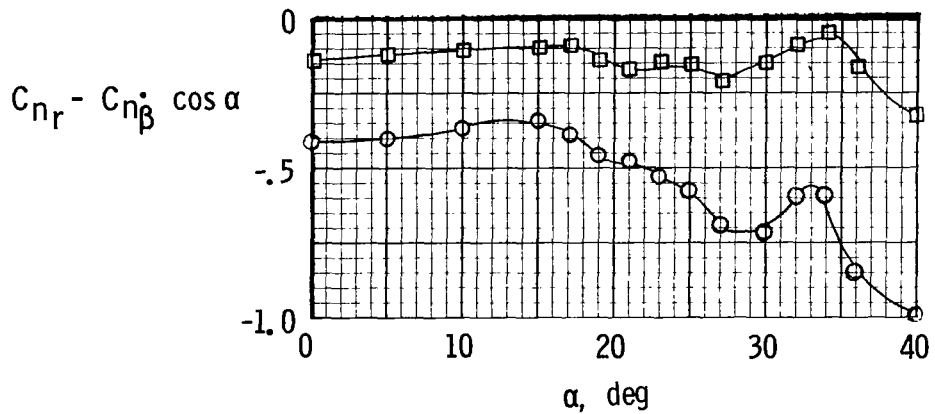
(b) Damping in yaw from forced-oscillation tests.

Figure 13.- Effect of vertical tail on yawing derivatives of a current fighter configuration.
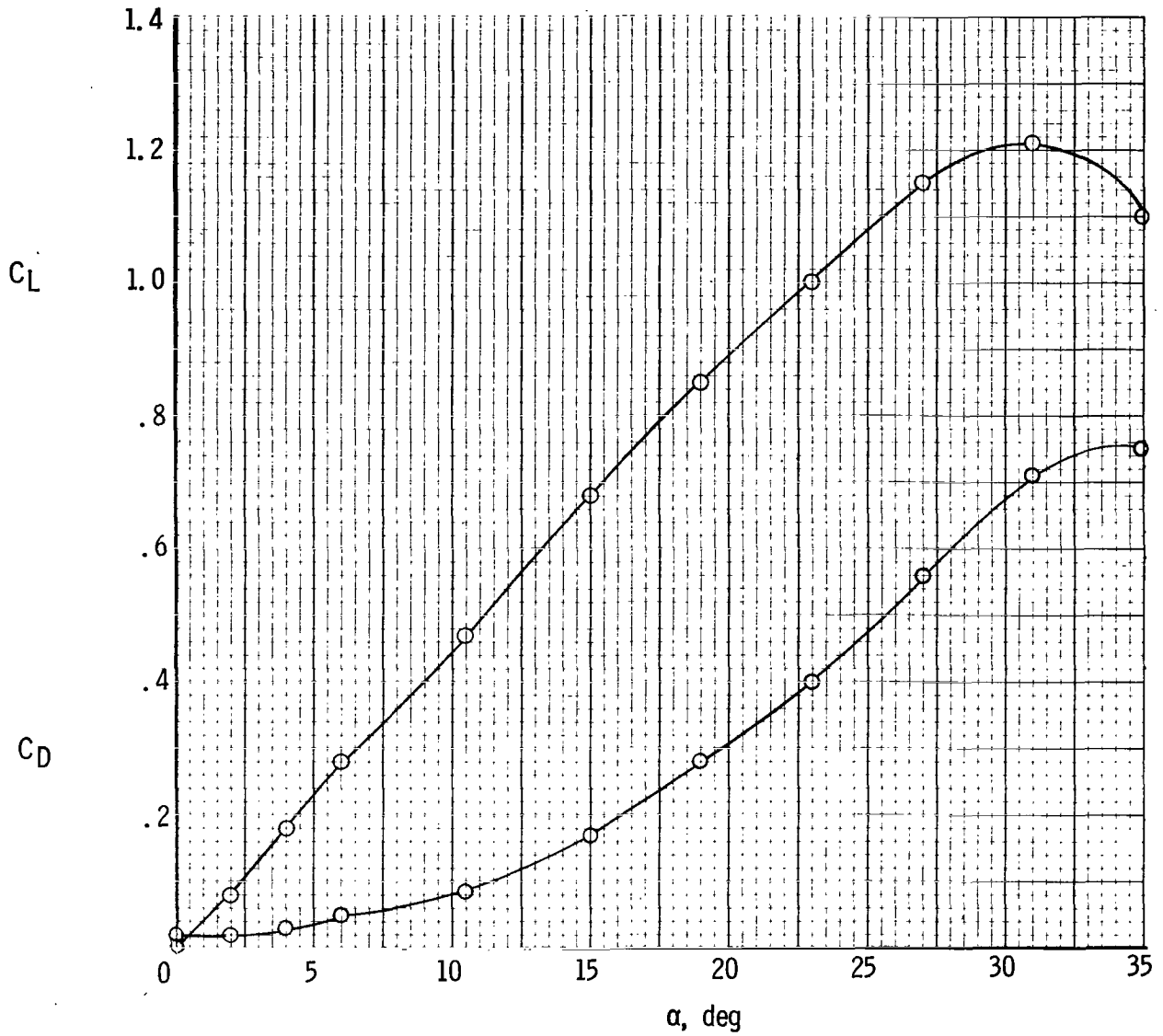
(a) Static longitudinal data (from ref. 17).

Figure 14.- Variation of aerodynamic characteristics with angle of attack for 60° delta-wing fighter configuration.
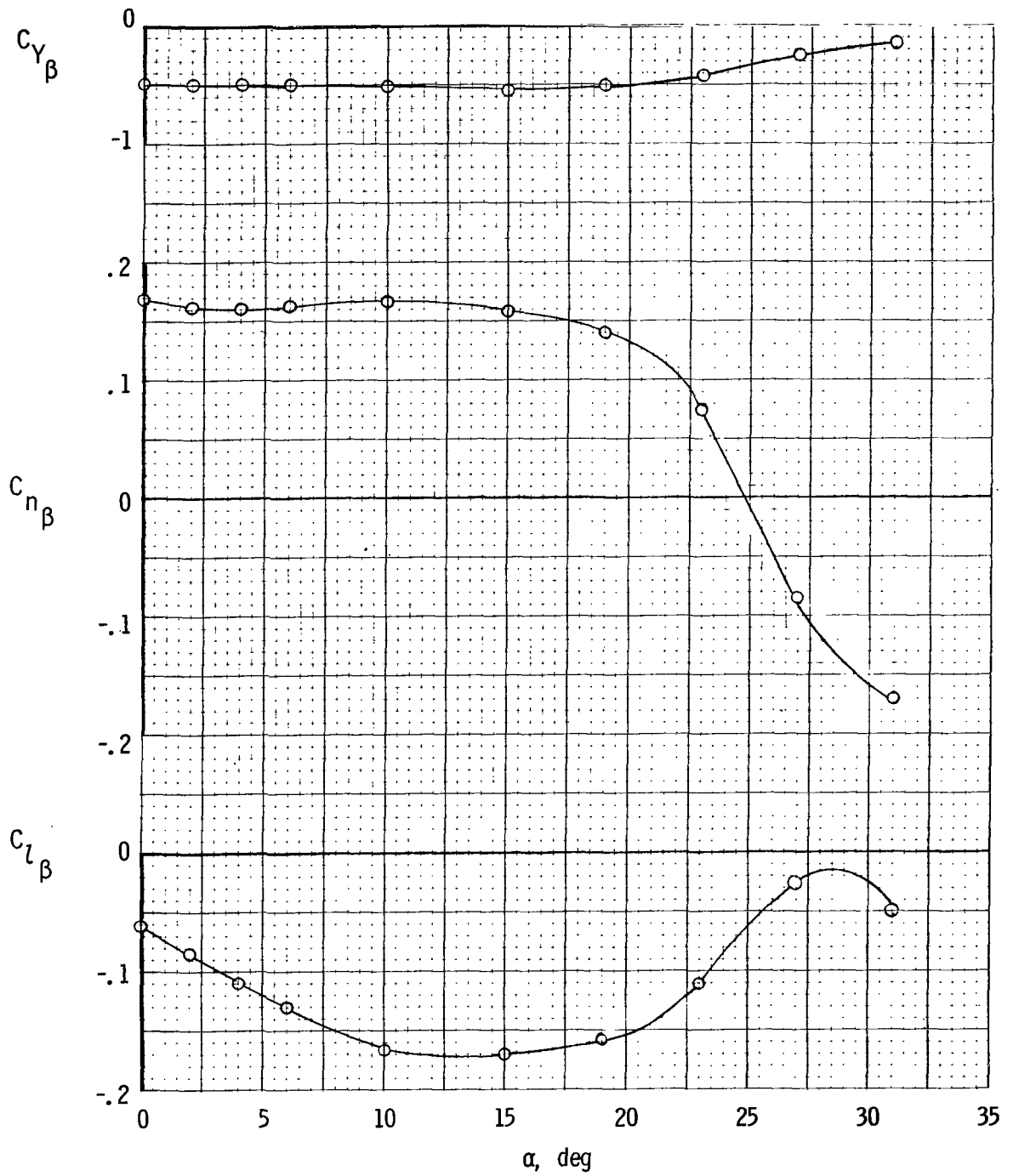
(b) Static lateral-directional stability derivatives (from ref. 17).

Figure 14.- Continued.
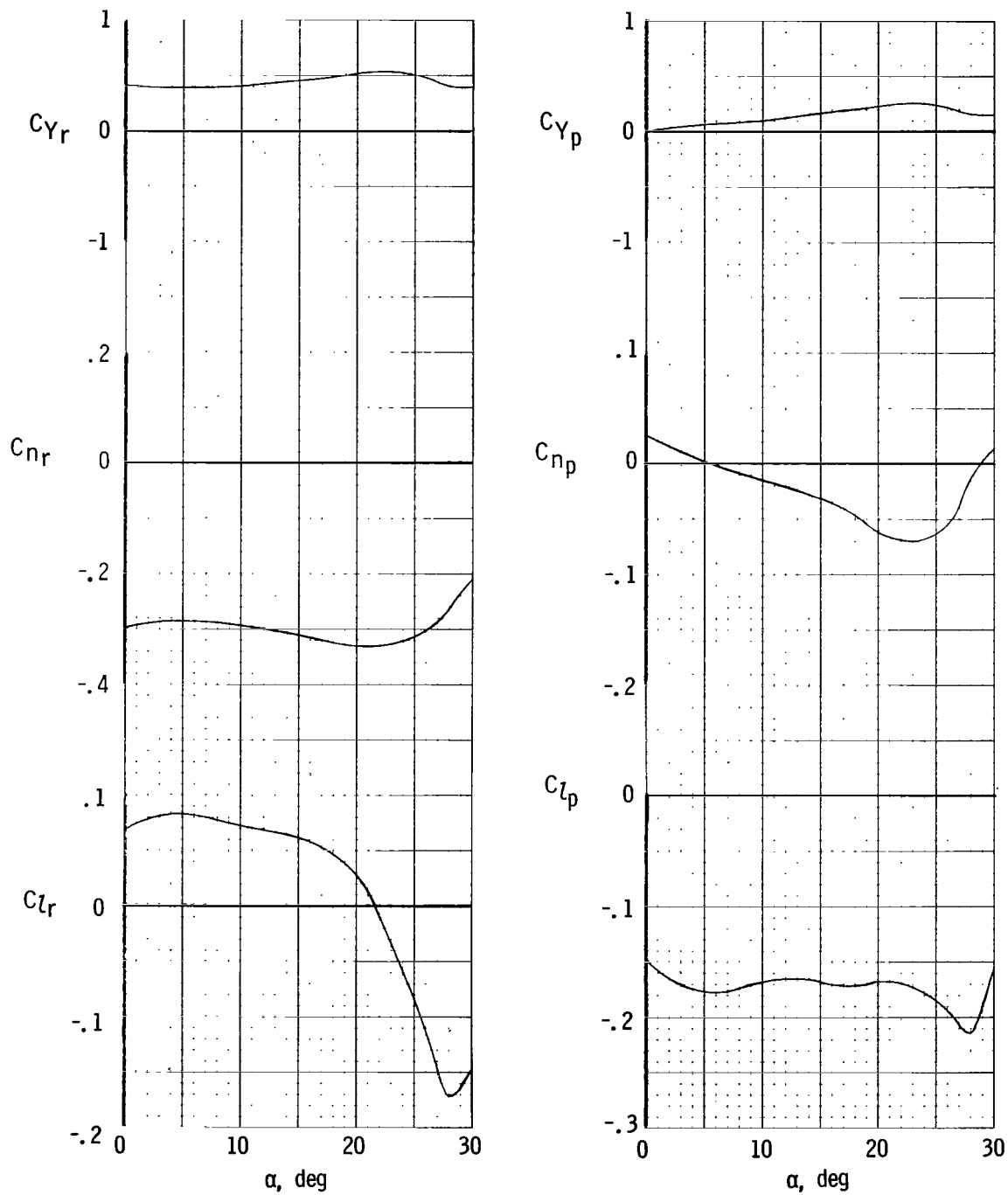
(c) Yawing and rolling stability derivatives (from refs. 17 and 18).

Figure 14.- Continued.
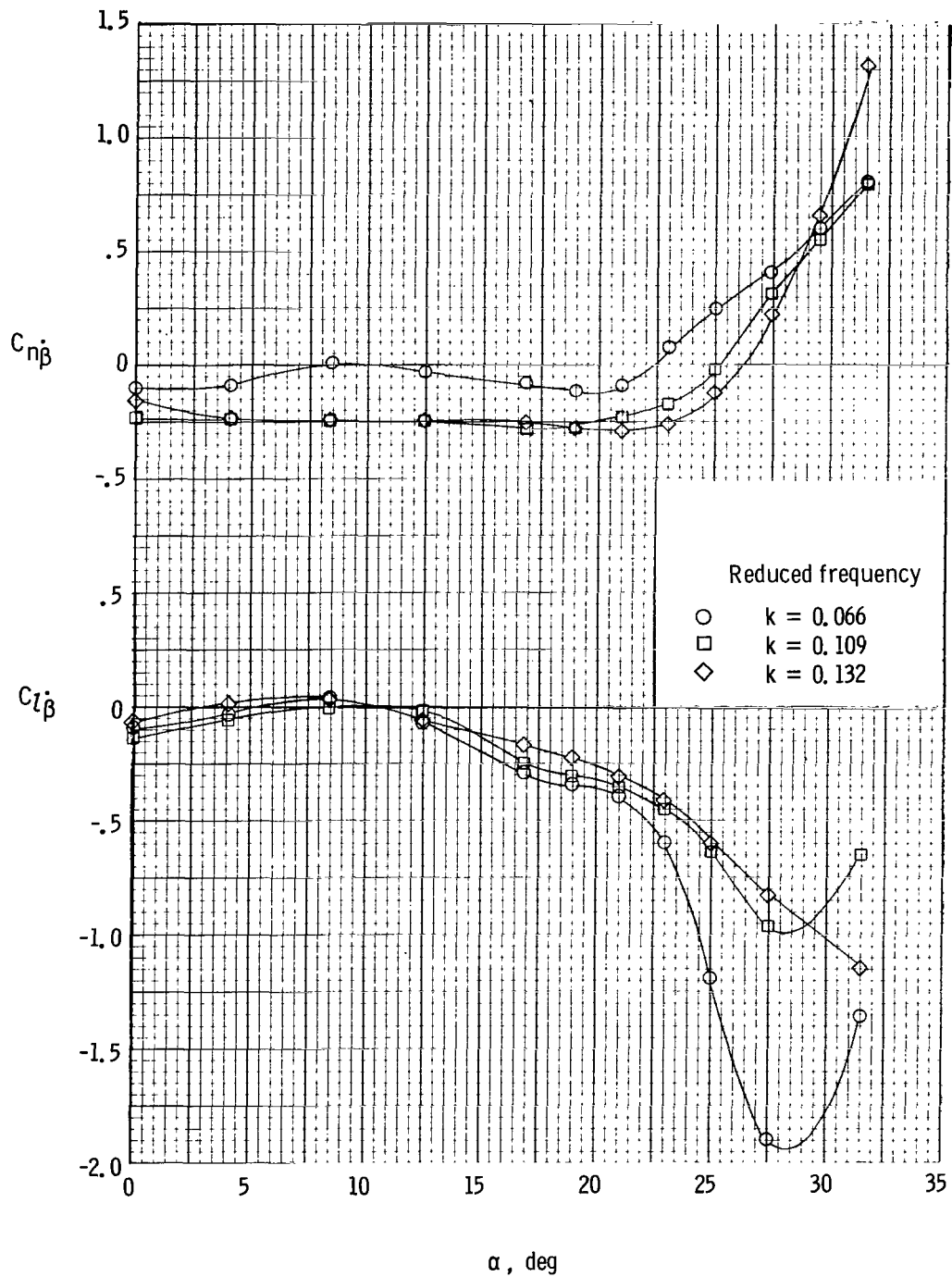
(d) Derivatives due to rate of change of sideslip (from ref. 4).

Figure 14.- Concluded.
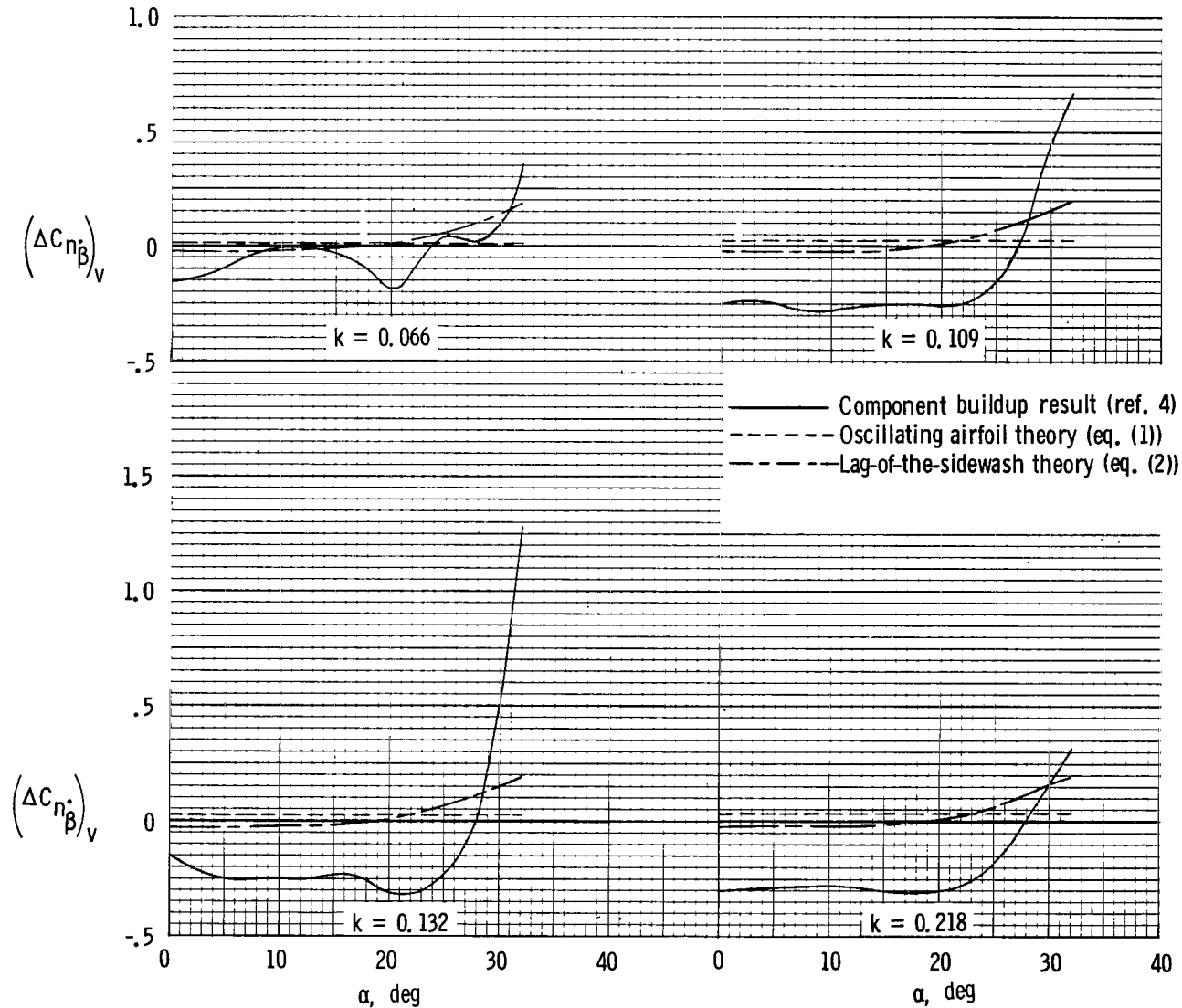
Figure 15.- Variation with angle of attack of vertical-tail contribution to $C_{n_{\dot{\beta}}}$ for delta-wing fighter configuration.
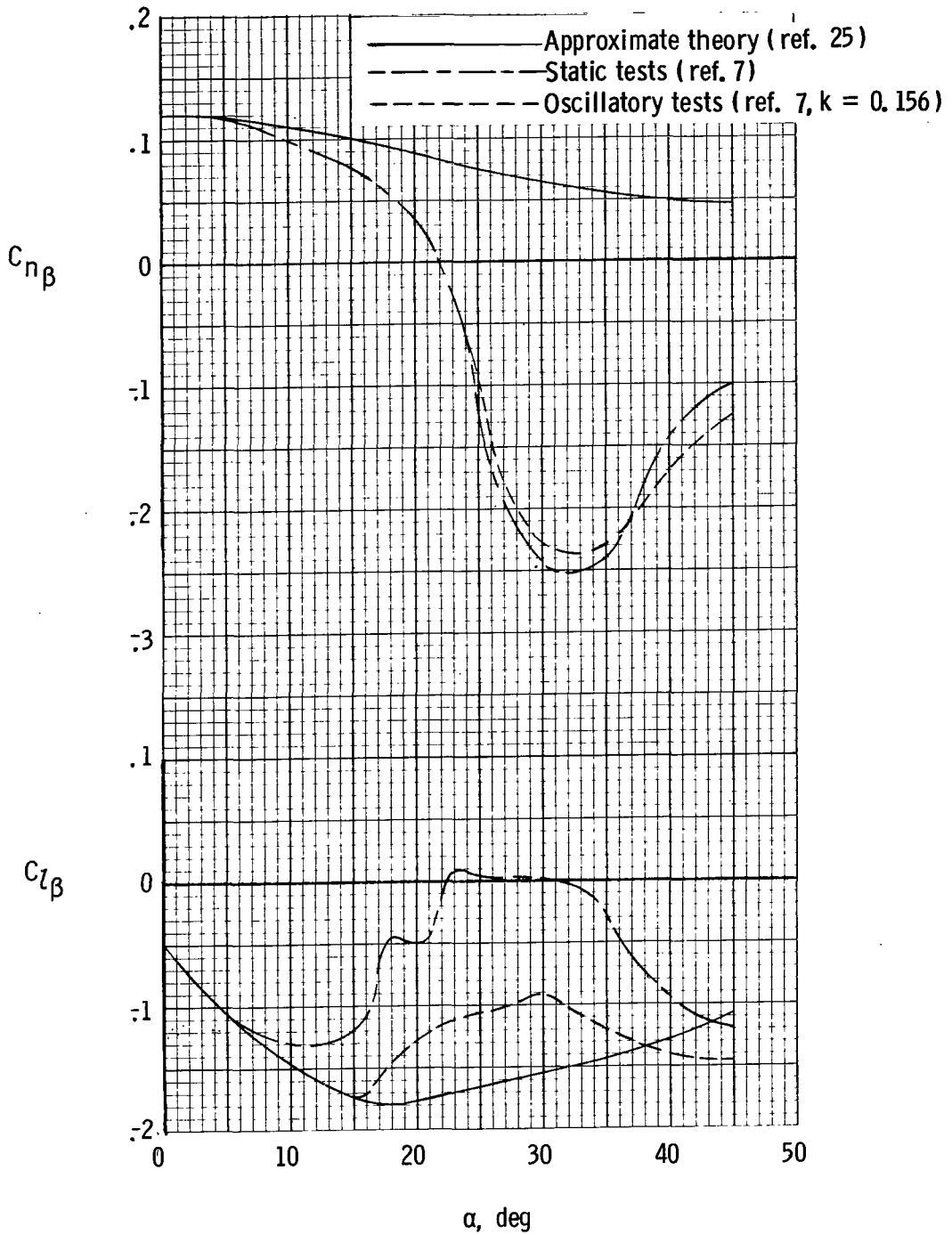
Figure 16.- Variation of static lateral-directional stability derivatives with angle of attack for twin-jet fighter airplane.
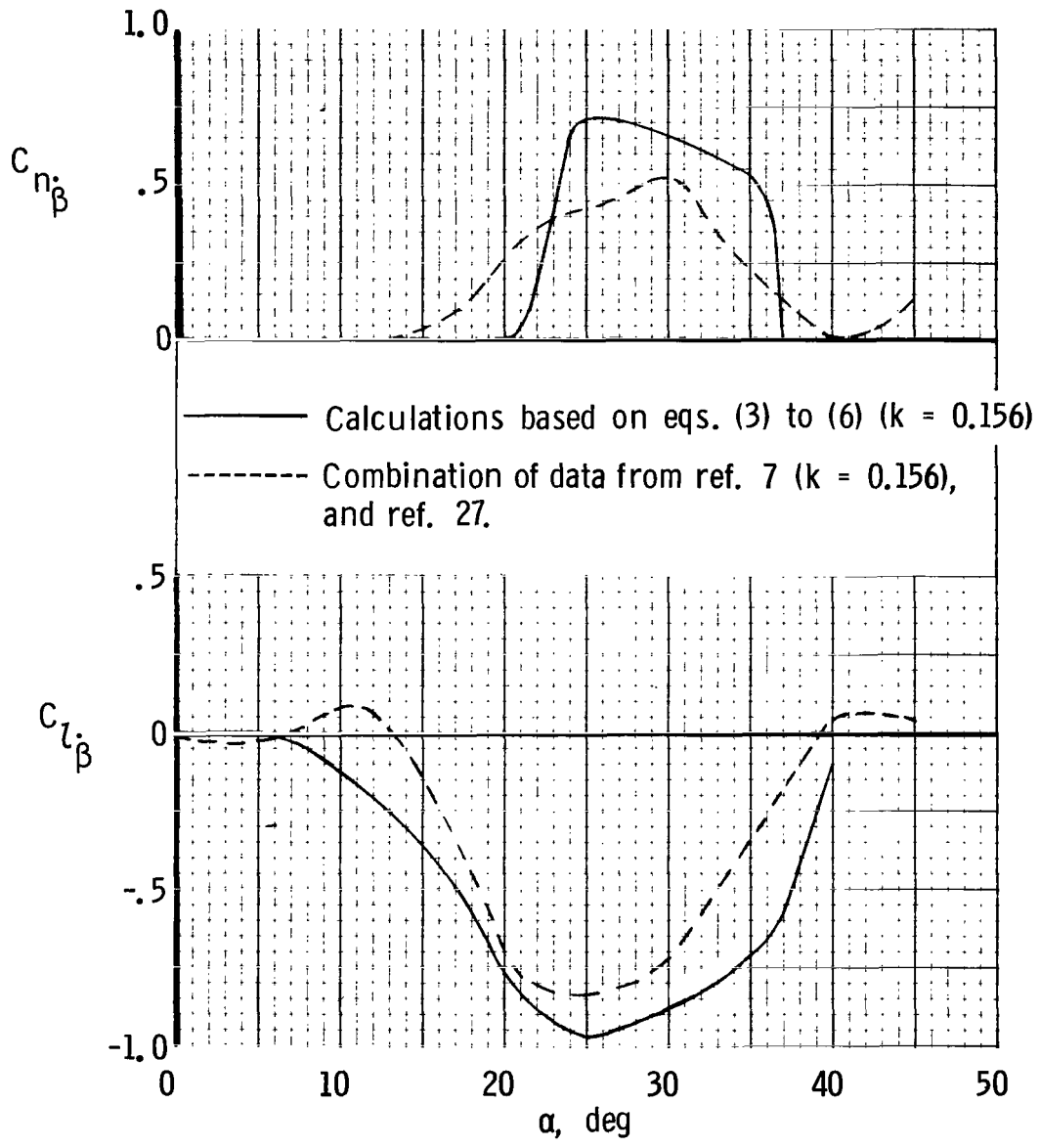
Figure 17.- Derivatives due to rate of change of sideslip for twin-jet fighter airplane.

"The aeronautical and space activities of the United States shall be conducted so as to contribute . . . to the expansion of human knowledge of phenomena in the atmosphere and space. The Administration shall provide for the widest practicable and appropriate dissemination of information concerning its activities and the results thereof."
    —NATIONAL AERONAUTICS AND SPACE ACT OF 1958

NASA SCIENTIFIC AND TECHNICAL PUBLICATIONS

TECHNICAL REPORTS: Scientific and technical information considered important, complete, and a lasting contribution to existing knowledge.

TECHNICAL NOTES: Information less broad in scope but nevertheless of importance as a contribution to existing knowledge.

TECHNICAL MEMORANDUMS: Information receiving limited distribution because of preliminary data, security classification, or other reasons. Also includes conference proceedings with either limited or unlimited distribution.

CONTRACTOR REPORTS: Scientific and technical information generated under a NASA contract or grant and considered an important contribution to existing knowledge.

TECHNICAL TRANSLATIONS: Information published in a foreign language considered to merit NASA distribution in English.

SPECIAL PUBLICATIONS: Information derived from or of value to NASA activities. Publications include final reports of major projects, monographs, data compilations, handbooks, sourcebooks, and special bibliographies.

TECHNOLOGY UTILIZATION PUBLICATIONS: Information on technology used by NASA that may be of particular interest in commercial and other non-aerospace applications. Publications include Tech Briefs, Technology Utilization Reports and Technology Surveys.

Details on the availability of these publications may be obtained from:

SCIENTIFIC AND TECHNICAL INFORMATION OFFICE

NATIONAL AERONAUTICS AND SPACE ADMINISTRATION
Washington, D.C. 20546